Understanding very faint X-ray binaries from X-ray light curves

Simon van Eeden
Supervised by Nathalie Degenaar

Anton Pannekoek Institute for Astronomy, University of Amsterdam
July 24, 2021

ABSTRACT

X-ray binaries known as accreting neutron stars and black holes include a selection of sources that appear as very faint having peak luminosity's of 10^{34-36} erg s^{-1}. Very faint X-ray binaries reach the limits of X-ray instrumental sensitivity which hampered detailed studies and therefore remain not fully understood. Possible explanations for their very faint character are that they have short orbital periods of a few hours or a different accretion process from bright sources. To find out more about the nature of these objects we have performed a first systematic analysis on accretion outburst light curves from 21 sources by determining the duration and decay time. We found that the distribution of the duration and decay time of each outburst appears very similar to bright X-ray binaries hinting to a similar accretion process. We have furthermore used the disc instability model to probe the accretion disc radius and orbital period and found short orbital periods of two to six hours for 6 sources. We have shown that the disc instability model can be used on outburst light curves that have sufficient number of observations. Therefore to further investigate the potential of this model we recommend to obtain sensitive X-ray observations each 1 to 3 days on new outbursts from very faint X-ray binaries.

VU VRIJE UNIVERSITEIT AMSTERDAM | UNIVERSITEIT VAN AMSTERDAM

Populaire samenvatting

Röntgendubbelster systemen bestaan uit een neutronen ster of een zwart gat en een donor ster die om elkaar heen draaien. Doordat neutronon sterren en zwarte gaten zo compact zijn kan hun extreme zwaartekracht materie van de buitenste lagen van de donor ster naar hen toe trekken. Hierdoor ontstaat er een stroom van materie richting het compacte object wat we ook wel accretie noemen. Deze stroom orienteerd zich dusdanig dat er een schijf met materie ontstaat rondom het compacte object. Door instabiliteit in deze schijf kunnen er uitbarstingen ontstaan waarbij in een aantal dagen tot weken erg veel materie op het compacte object valt. Tijdens een uitbarsting wordt er veel meer röntgenstraling uitgezonden en dat kunnen we met röntgen telescopen in de ruimte zoals Swift en RXTE waarnemen.

In dit onderzoek is gekeken naar 21 röntgendubbelster systemen die erg zwak zijn. We weten tot nog toe niet waarom deze systemen zo zwak zijn. Mogelijke verklaringen hiervoor zijn dat vergeleken met heldere bronnen de omlooptijd veel kleiner is of dat de accretiestroom heel anders is. Om dit beter te begrijpen hebben we van deze systemen het helderheidsverloop van uitbarstingen gekarakteriseert, iets wat tot nu toe alleen nog voor heldere bronnen gedaan is. Als eerst hebben we gekeken of uitbarstingen van deze bronnen een andere lengte en afvaltijd hebben in vergelijking met heldere bronnen. We hebben gevonden dat de distributie van de lengte en de afvaltijd in hele zwakke systemen dezelfde trend volgt als die van heldere systemen. We denken dat dit een indicatie geeft dat hele zwakke systemen hetzelfde accretie process volgen als heldere systemen.

Ten tweede hebben we gebruik gemaakt van een stabiliteits model om de omlooptijd van het systeem te kunnen bepalen omdat we verwachten dat deze korter is voor zwakkere systemen. Echter geldt voor veel hele zwakke bronnen dat het helderheidsverloop van een uitbarsting niet altijd duidelijk te bepalen is omdat ze zo zwak zijn maar ook omdat er soms dagen tot een week tussen twee observaties kan zitten. Het model lijkt voor zes systemen die een duidelijk helderheidsverloop laten zien de uitbarsting vorm goed te benaderen. Alle zes systemen hebben een kortere omlooptijd van 2 tot 6 uur wat overeenkomt met een van de verwachtingen. Dit geeft ons ook een indicatie voor een vergelijkbaar accretieprocess in hele zwakke en heldere systemen. Voor 2 bronnen geeft het model resultaten die overeenkomen met onafhankelijke observaties. Dit suggereert dat het model gebruikt kan worden om meer te weten te komen over de accretie eigenschappen van hele zwakke systemen. Om dit verder te onderzoeken zijn er meer observaties in X-ray nodig waarbij gekeken wordt met een observatie interval van ongeveer een dag zodat het helderheidsverloop duidelijk te zien is.

1 Introduction

The majority of all stars are part of a binary system in which two stars orbit the center of mass. A special case of binary systems are X-ray binaries which contain a neuron star (NS) or a black hole (BH) and a donor star. The strong gravitational forces from these compact objects can cause accretion of matter from the donor star on to the compact object (shown in figure 1).

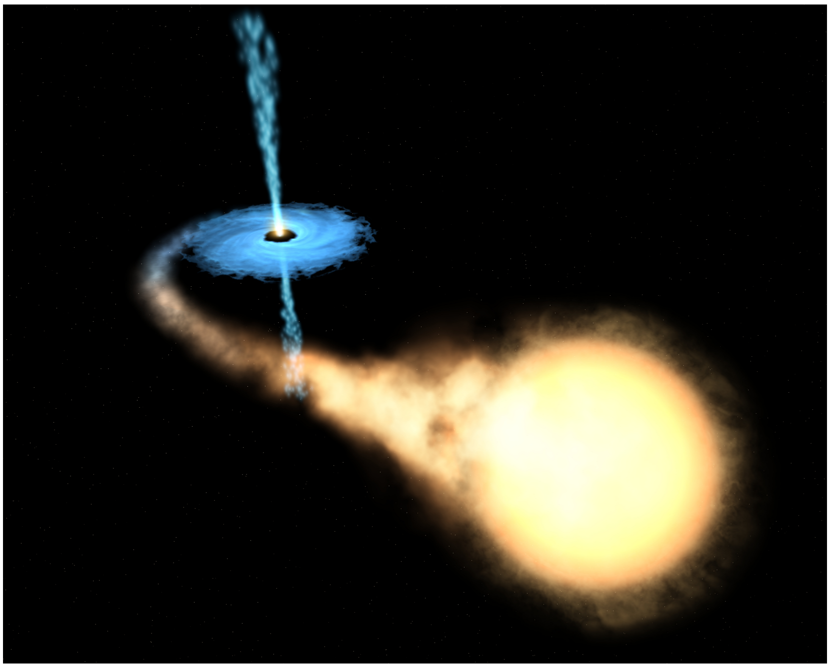

Fig. 1: Artist impression of an accreting X-ray binary.

During accretion gravitational potential energy is converted into radiation mostly in X-rays which can be observed with X-ray telescopes. Observations have shown persistent sources that have a continuous accretion rate and emit continuous X-rays. However they also show transient sources that are most of the time in quiescence with little accretion and occasionally show a rise in X-ray. These occasional events are called outbursts and typically last for a couple of days to several months while reaching peak luminosity's up to 10^{39} erg s^{-1}. Outbursts are caused by thermal-viscous instabilities in the accretion disc described by the disc instability model (Lasota 2001; Hameury 2020). Currently roughly 200 X-ray binaries have been observed (see Liu et al. 2007 for an overview up to 2007, with a few systems discovered since then). Since the last 15 years evidence have grown for the existence of Very Faint X-ray Binaries (VFXBs) that have outburst peak luminosity's of 10^{34-36} erg s^{-1} 2-10 keV (Wijnands et al. 2006). For a long time, detailed studies on this subclass were difficult because their faintness approaches the instrumental sensitivity limits. Despite the observational difficulties currently about 30 X-ray binaries are classified as a VFXB.

It is yet not understood why VFXBs are so faint. Two possible explanations for there faintness are that they have short orbital periods (King and Wijnands 2006; in 't Zand, J. J. M. et al. 2007; Wu et al. 2010; Hameury and Lasota 2016) or a different accretion process (Heinke et al. 2009; Degenaar et al. 2014; Heinke et al. 2015) compared to bright X-ray binaries. So far research have been focusing only on individual sources but to find out more about the origin of the faint character it is worthwhile to perform a systematic analysis on outburst light curves from multiple VFXBs. There have been already systematic studies of outbursts from bright X-ray binaries (24 sources in Chen et al. 1997; 36 sources in Yan and Yu 2015) in which they determined distributions for the e-folding rise and decay timescale, duration and total radiated energy of each outburst. Comparing outburst characteristics such as the duration and decay time of VFXBs with those of bright sources can provide us more insight in potential differences in the accretion process of these two sub classes.

So far the disc instability model has described the decay shape of several outbursts from bright sources (Powell et al. 2007 on ten sources, one of them shown in figure 2) and for a handful of VFXBs (Heinke et al. 2015 on two sources) it has proved to be a tool to test if VFXBs have short orbital periods. It is therefore interesting to test the disc instability model on more VFXBs and find out if they have short orbital periods.

To fulfill these needs in exploring the nature of very faint x-ray binaries, we aim to answer the following two questions. What is the typical duration and decay time of outbursts of VFXBs? Do VFXBs have shorter orbital periods?

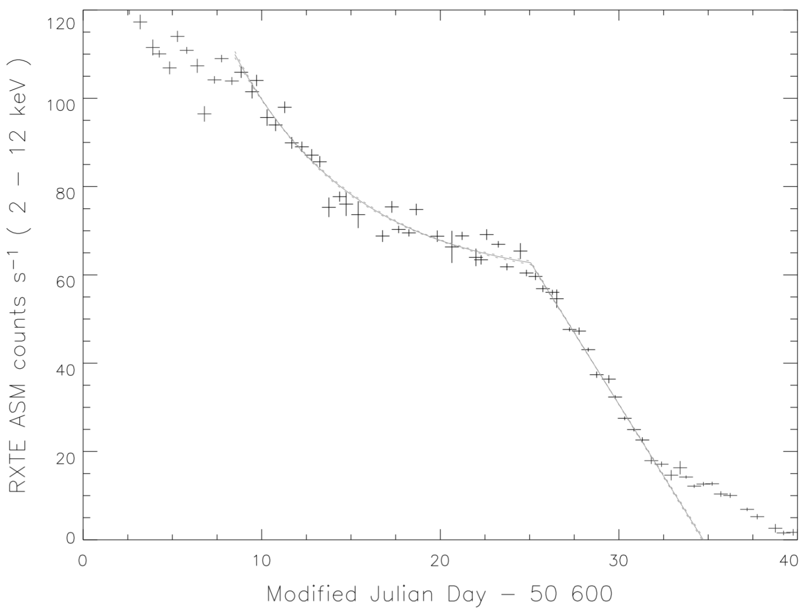

Fig. 2: The light curve of GRO J 1655-40 fitted to the disc instability model, from Powell et al. 2007.

2 X-ray binary classification

This section contains the required background knowledge in the classification of X-ray binaries. The classification of X-ray binaries involves three criteria: the type of the compact object, the mass of the companion star and the X-ray peak luminosity. The following sections will explain each criteria.

2.1 Type of the compact object

Black hole

The first classification criteria is the type of compact object; BH or NS. BHs can be identified by the mass of the compact object. If in NSs the mass becomes higher then $\sim 2.5 - 3M_{\odot}$ depending on the equation of state (Baiotti et al. 2008), the neutron degeneracy pressure can not balance the gravitational force anymore. Therefore if the mass of the compact object exceeds a critical mass of $\sim 2.5 - 3M_{\odot}$ the compact object must be a BH. Calculating the mass of the compact object with spectral analysis can be a hard task because in order to identify the spectra of the donor star the X-ray binary must be bright enough in quiescence. If this is the case the orbital period can be extracted from a radial velocity curve from the donor star. The radial velocity curve originate from the fact that if the orbital plane is aligned with our line of sight the spectral lines are blue shifted when the donor star moves towards us and red shifted when the donor star moves away from us. Knowing the period, assuming that the inclination is 90 degrees and the mass of the donor star is zero the mass function from Kepler's laws gives the minimum mass of the compact object. If this mass exceeds $3M_{\odot}$ the compact object must be a BH. This method resulted in the identification of several tens of BH X-ray binaries (Corral-Santana et al. 2016; Tetarenko et al. 2016) with XTE J1118+480 as VFXB (Torres et al. 2004).

Neutron star

In contrast to a BH that has a event horizon, a NS has a solid surface and a magnetic field which give rise to thermonuclear X-ray bursts (Cornelisse et al. 2002) and X-ray pulsations (Ng et al. 2021). During a thermonuclear burst material piles up at the surface and eventually detonates resulting in a bright and short flash in X-ray (shown in figure 3).

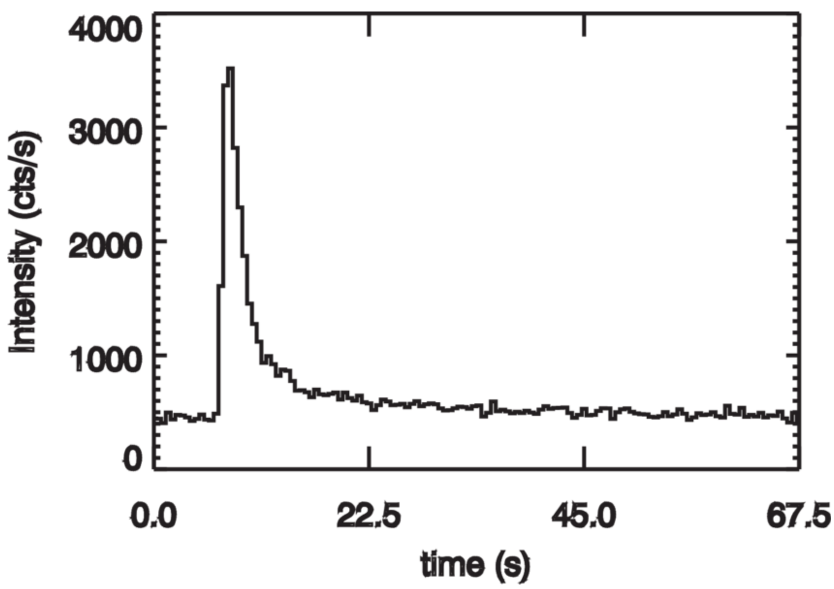

Fig. 3: Example of a typical thermonuclear burst observed in 4U 1735 - 445 (Tournear et al. 2008).

X-ray pulsations originate from the magnetic field in combination with the spin of a NS. The magnetic field forces material from the accretion disc to move along the magnetic field lines and end up at the magnetic poles. While material falls onto the poles they heat up and shine brighter which causes X-ray pulsations when the NS spins in our line of sight.

2.2 Mass of companion star

Low mass or high mass X-ray binaries
High mass X-ray binaries (HMXBs) can accrete material by a stellar wind or decretion disc of the companion star. Be/X-ray binaries are the most common type for accretion via a decretion disc. These systems harbor a B or O type star that spin so fast that the rotational force overcomes the gravitational force and a decretion disc forms (Okazaki and Negueruela 2001). HMXBs can also host a supergiant star that loses mass by a strong stellar wind. The material that is lost can be captured and accreted onto the compact object. In low mass X-ray binaries (LMXBs) mass transfer happens typically via Roche Lobe overflow during which a accretion disc forms around the compact object (see section 3 for more detail).

2.3 Luminosity

Bright
The third classification of X-ray transients is based on their X-ray peak luminosity when they are in outburst. Bright to very bright X-ray binaries have peak luminosity's of 10^{36-39} erg s^{-1} 2-10 keV. Currently the best description of the accretion behaviour of LMXBs in this class is given by the disc instability model explained in section 3. A large fraction of this subclass contain NSs and they are more concentrated towards the galactic center (Cornelisse et al. 2002) but the latter might be a consequence of observations mainly focusing on this region (Degenaar and Wijnands 2009).

Very Faint
Very Faint X-ray binaries have peak X-ray luminosity's of 10^{34-36} erg s^{-1}. There have been several suggestions for explaining the very faint character. They could be intrinsically bright but appear as very faint due to their large distance (Wijnands et al. 2006). Another option could be a edge-on oriented accretion disc that partly blocks X-rays (Muno et al. 2005). This way it appears as a very faint source but has a intrinsic luminosity that belongs to a bright source. Although, it is more likely that most VFXBs have a very faint intrinsic luminosity (Wijnands et al. 2006). As Wijnands et al. 2006 mentioned, different characteristics have been found in the analysis of light curves and spectra from VFXBs and it seems to be a inhomogeneous class including LMXBs and HMXBs, and with the distinction between bright and very faint rather arbitrary. However we currently know that most sources in this class are LMXBs and those are studied here.

3 The disc instability model

In LMXBs accretion happens via Roche lobe overflow. While material from the outer layers of the companion star is transferred towards the compact object angular momentum must be conserved and a accretion disc forms (Frank et al. 2002). Instabilities in this accretion disc can trigger the rise of outbursts. The disc instability model is the accepted description of outbursts in LMXBs (King and

Ritter 1998). This model includes the effects of the disc irradiation on the disc stability caused by intense X-rays from the inner disc and for NSs the stellar surface may contribute as well.

The disc instability model provides predictions for the outburst decay shape depending on the ionization state of the accretion disc. At the start of every outburst the accumulation of matter in the accretion disc is able to ionize the disc. The ionization raises the disc's viscosity which causes rapid rise in X-ray flux. When the accretion disc is fully ionized by irradiation from the central source a exponential decay is predicted. As soon as the outer edge of the disc cools down below the hydrogen ionization temperature the accretion disc becomes partly ionized. During this stage a linear decay is expected until it fades to quiescence. The transition from exponential to linear decay happens at a luminosity

$$L_t(NS) = 3.7 \times 10^{36} R_{11}^2 \mathrm{erg\ s}^{-1} \tag{1}$$

for NSs and

$$L_t(BH) = 1.7 \times 10^{37} R_{11}^2 \mathrm{erg\ s}^{-1} \tag{2}$$

for BHs with R_{11} the accretion disc radius in units of 10^{11} cm and L_t the transition luminosity (Shahbaz et al. 1998). The difference is due to whether the stellar surface or the inner disc is the dominating source of irradiation. Section 4.3 provides a explanation of how physical parameters were extracted from this model.

4 Method

From the about 30 known VFXBs we selected light curves that show a outburst and have enough data points to reveal a outburst shape. The selected X-ray light curves cover data from two telescopes that are sensitive enough to detect outbursts in VFXBs and allow for daily observation intervals: the Rossi X-ray Timing Explorer (*RXTE*) which observed from 1996 until 2012 and the Neil Gehrels Swift Observatory (*Swift*) which is observing since 2005. All the light curves from *RXTE* contain continuous observations taken with the All Sky Monitor (*ASM*) [1] or with the the Proportional Counter Array (*PCA*) [2] (Swank and Markwardt 2001). The *PCA* and *ASM* have a energy range of 2–10 keV.

Six *Swift* light curves are from the galactic center observing campaign (Degenaar et al. 2015). The other *Swift* light curves are processed via the online tool from Evans et al. 2007. All *Swift* light curves contain series of observations typically triggered by reports of source activity. The X-ray telescope on board of *Swift* has two observing modes. Most of the time our sources are weak enough to be observed with the Photon Counting (*PC*) mode but when the count rate reach a critical value of $\sim$1 c s^{-1} pile-up becomes an issue and *Swift* switches to Window Timing (*WT*) mode. In both modes the X-ray telescope on board *Swift* is sensitive to a energy range of 0.3-10 keV. For the analysis on the *Swift* light curves we have used data from both observing modes.

4.1 Outburst duration τ_{dur}

Based on the symmetry of most outburst shapes, each outburst is fitted to a Gaussian to determine the outburst duration using the `astropy` package (Astropy Collaboration and Robitaille 2013). From each Gaussian fit the standard deviation (σ) is used to derive the duration of the outburst by applying

$$\tau_{dur} = 6\sigma \tag{3}$$

[1] http://xte.mit.edu/asmlc/ASM.html
[2] https://asd.gsfc.nasa.gov/Craig.Markwardt//galscan/main.html

with τ_{dur} the outburst duration and σ the standard deviation from the Gaussian fit. On most outbursts a Gaussian does not fit perfectly but it does provide a systematic way to roughly estimate the duration. In order to get the best possible fit we have extracted the average count rate and the standard deviation from fluctuations around the zero point:

1. **Fit-data selection**
   The standard deviation of fluctuations around the zero point is used as a threshold for noise detection in the following way. For each outburst, data points were selected from the peak to earlier and later times until two adjacent observations have count rates below 2σ. This selected region is used as the input data for the Gaussian fit. For some *Swift* light curves containing solely the outburst region we used all data points.

2. **Offset count rates**.
   In order to get the best possible fit the light curve should converge to a average count rate of zero at earlier and later times similar to the Gaussian. Therefore all the light curve is subtracted by the average count rate of the fluctuations around the zero point. Light curves that only show the outburst region weren't corrected for zero point fluctuations.

For outbursts containing a few data points ($\sim$4) `astropy` can have trouble in finding the best fit and converge to amplitudes bigger then ten times the peak count rate. To avoid this behaviour and still be able to estimate the duration of these outbursts the amplitude is constrained to

$$\text{amplitude} < 1.3 \times \text{peak rate} \tag{4}$$

4.2 Outburst decay time τ_{dec}

The second outburst parameter that is determined is the decay time τ_{dec}, also referred to the e-folding timescale computed over the outburst decay region (Chen et al. 1997). The decay time is, such as the duration, unrelated to instrumental sensitivity which makes it suitably for comparison between different sources from different telescopes. In order to extract the decay time from each outburst, a exponential function was fitted with the `astropy` package. The exponential fit function is defined as

$$F(t) = A \exp\left(-\frac{t}{\tau_{dec}}\right) \tag{5}$$

with $F(t)$ the count rate, A the amplitude, t the time after the start of the outburst decay and τ_{dec} the decay time. As mentioned earlier, we fitted this decay model to the outburst decay region. This region is determined similarly as for τ_{dur} but the start point is fixed at the time of the peak count rate. For some *Swift* light curves that are containing solely the decay region the whole data set was used.

The fit function 5 converges to zero moving forward in time. So to obtain the best fit the fluctuations around the zero point should have a average count rate of zero. This correction is performed by subtracting the average of the zero point fluctuations similar to τ_{dur}.

4.3 Decay model

We have used the accretion disc model described in Heinke et al. 2015 to fit outburst decay light curves. Therefore we applied python code[3] that contains all of the following. At the beginning of the

[3] Thanks to Dr. Arash Bahramian

outburst decay when the disc is completely ionized the light curve shows a exponential decay shape described by

$$F(t) = (Ft - Fe)\exp\left(-\frac{t - t_t}{\tau_e}\right) + F_e \tag{6}$$

with $F(t)$ the count rate, F_t the count rate at the transition, F_e the exponential amplitude, t the time, τ_e the exponential decay time and t_t the time at the transition. The exponential amplitude is constrained to $0.4L_t \leqslant L_e \leqslant L_t$ based on Heinke et al. 2015. At some time t_t the irradiation cannot maintain a fully ionized disc and the decay shape switches to linear described by

$$F(t) = F_t\left(1 - \frac{t - t_t}{\tau_l}\right) \tag{7}$$

with $F(t)$ the count rate, F_t the count rate at the transition, t the time, t_t the time at the transition and τ_l the linear decay time. The final model thus looks like:

$$F(t) = \begin{cases} (6), & t \leqslant t_t. \\ (7), & t > t_t. \end{cases} \tag{8}$$

The model is fitted using Markov Chain Monte Carlo (*MCMC*) sampling. This is an improved version of the basic Monte Carlo sampling that produces a probability distribution from random start variables. The *MCMC* gives a probability distribution for each of the five parameters. Each parameter range is constrained by values matching with the outburst count rates. The probability distribution lies between this chosen range and the meridian of the distribution is taken as the best fit value.

Source selection

In order to fit this model to an outburst decay, the transition from a exponential to a linear decay must be clearly visible. In addition the number of data points at each side of the transition must be such that the difference between a totally exponential or linear decay is clear. For example some *Swift* light curves (see appendix 8.1) are having data points with intervals of one week which can't be used. However most *RXTE* light curves have intervals of one day for which it is possible to distinct the exponential and linear part. In total 7 outbursts light curves from 6 sources meet these requirements and are fitted with the decay model.

Accretion disc radius R_{circ}

With the fit parameters from this model several physical properties of the binary system can be derived. The first one is the radius of the accretion disc. This can be derived from

$$R_{disc} = 3.5 \times 10^7 \sqrt{\tau_e} \tag{9}$$

with R_{disc} the accretion disc radius and τ_e the exponential decay time (Heinke et al. 2015).

Orbital period P_{orb}

The second physical property that is determined is the orbital period P_{orb}. This orbital period is derived from the disc radius R_{disc} and the mass fraction q defined as the mass of the companion star divided by the mass of the compact object:

$$P_{orb} = 3\left(\frac{R_{disc}}{R_\odot}\right)^{3/2} \frac{1}{(1+q)^2} \frac{1}{[0.500 - 0.227\log(q)]^6}\mathrm{h} \tag{10}$$

with $R_\odot$ the mass of the Sun (Heinke et al. 2015).

Model validation
For sources with a known distance d we are able to check if the model is corresponding to the theory with F_t. Therefore we converted count rates into flux with the Portable, Interactive Multi-Mission Simulator (*PIMMS*) tool (Mukai 1993)[4]. By replacing L_{acc} in equation 11 with the theoretical value from equations 1 or 2 and using the transition flux F_t from the fit we estimated the distance.

$$L_{acc} = 12\pi F d^2 \tag{11}$$

5 Results

5.1 Outburst detection

In total we found 41 outbursts in 21 sources listed in table 1. For each source we noted their compact object type: BH, candidate black hole (cBH), NS or candidate neutron star (cNS) in column 2. Sources with unknown compact object type are labeled with question mark. For each outburst the telescope used for observation and the time at the peak of the outburst is noted in column 2 and 3 respectively.

In total 5 outbursts were classified as unsuitable to determine the duration or decay time via fitting, their light curves can be found in the appendix 8.1:

- Two sources, IGR J17597-2201 and XTE J1744-230, contain outbursts with variable count rates longer than one year, they are classified as quasi persistent (QP) outbursts. These QP outbursts result in a unclear decay shape hence it is hard to determine their duration or decay time.

- The light curve of IGR J17451-3022 also shows high variability in outburst which hampered good approximations of the duration and decay with our method.

- The *Swift* light curve of SAX J1828.5-1037 shows a clear outburst at MJD 55875 but only contains data points at the peak of the outburst. Therefore the duration or decay time of this outburst cannot be determined.

- XTE J1719-356 shows one clear enhancement in count rate at MJD 55376 in the *RXTE* light curve. The *Swift* light curve contains increased activity around the same time (Armas Padilla et al. 2010) shown in figure 4, which indicates that the increased activity in the *RXTE* light curve is real. Despite this increased activity, in the *RXTE* light curves there is now outburst shape visible besides this single data point. Additionally the *Swift* light curve does not show a clear outburst shape also due to the limited number of data points. This makes it too hard to conclude anything about the duration or decay time of this outburst.

- Five outbursts (MJD 58584 XTE J1728-295, MJD 56010 IGR J1817-3656, MJD 55595 Swift J1357.2-0933, MJD 57868 Swift J1357.2-0933 and MJD 54644 XMMJ174457-2850.3) weren't fit to a Gaussian because they only contain the decay part.

- The outburst of IGR J17375-3022 at MJD 52466 has too few data points to resolve the outburst decay shape and produces a nonphysical decay time of 0.01. So this outburst decay time was excluded for analysis.

[4] https://heasarc.gsfc.nasa.gov/cgi-bin/Tools/w3pimms/w3pimms.pl

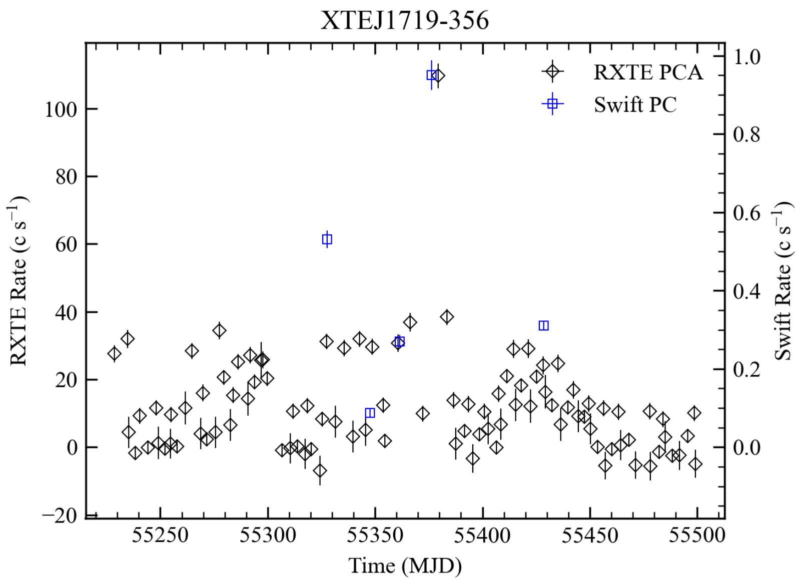

Fig. 4: The *RXTE* and *Swift* light curve of XTE J1719-356 show increased activity around MJD 55377 indicating that there is a outburst.

5.2 Duration

In total 36 outbursts were successfully fitted to Gaussian function. As an example, we show in figure 5 a Gaussian fit of an outburst in XTE J1728-295. All other fits can be found in the appendix 8.2. The duration extracted from the fits is shown in column 5 of table 1. We found an average outburst duration of 55.0 days and a median of 24.6 days. The distribution of the duration from all outbursts can be seen in figure 7. From the distribution can be seen that BHs tend to have longer outbursts than NSs.

5.3 Decay time

In total 40 outbursts were successfully fitted to a exponential function. As an example, we show in figure 6 a exponential fit of an outburst in XTE J1728-295. All other fits can be found in the appendix 8.3. The decay time extracted from the fits is shown in column 5 of table 1. We found an average outburst decay time of 11.9 days and a median of 4.7 days. The distribution of the decay time from all outbursts can be seen in figure 8. From the distribution can be seen that similar to the duration BHs tend to have longer decay times than NSs.

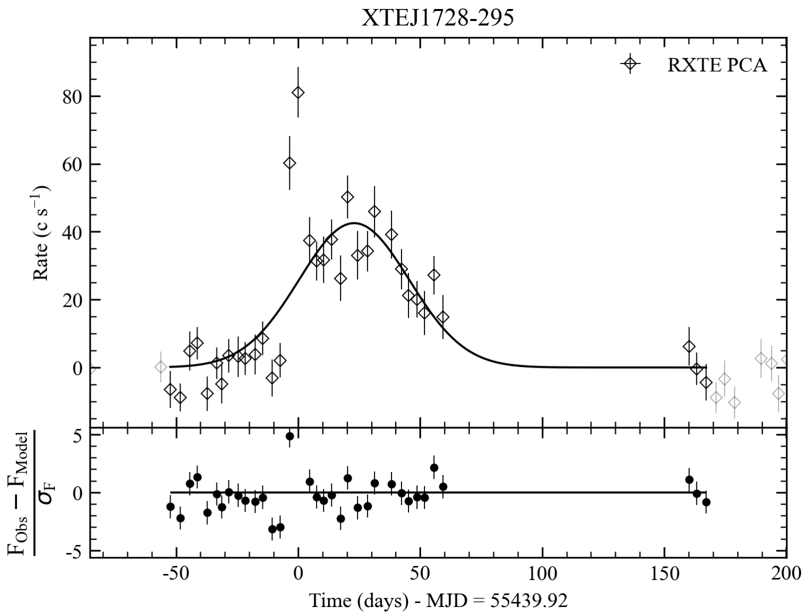

Fig. 5: Gaussian fit of an outburst from XTE J1728-295 taken with the PCA on board RXTE. The bottom subplot shows the fit error (F_{Obs}-F_{Model}) divided by the light curve error (σ_F) and for each data point a 1σ error bar.

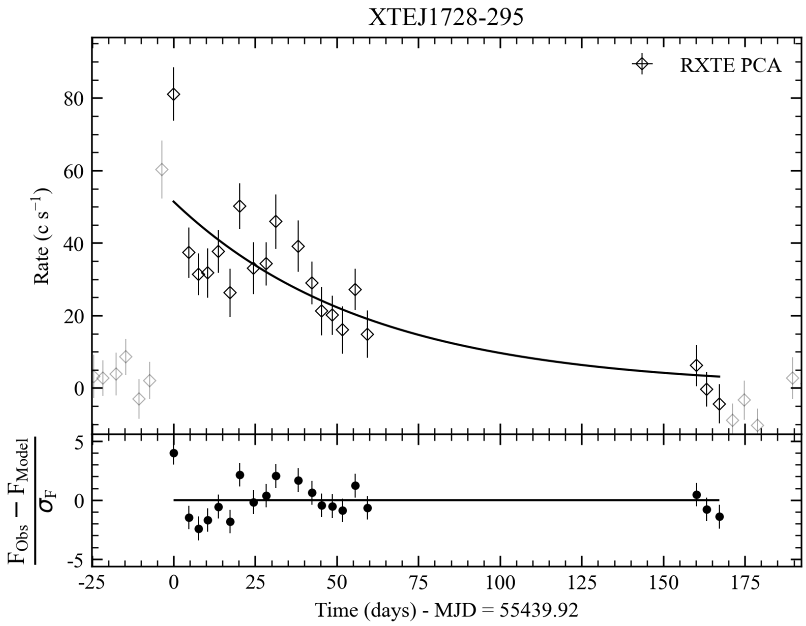

Fig. 6: Exponential fit of an outburst from XTE J1728-295 taken with the PCA on board RXTE. The bottom subplot shows the fit error (F_{Obs}-F_{Model}) divided by the light curve error (σ_F) and for each data point a 1σ error bar.

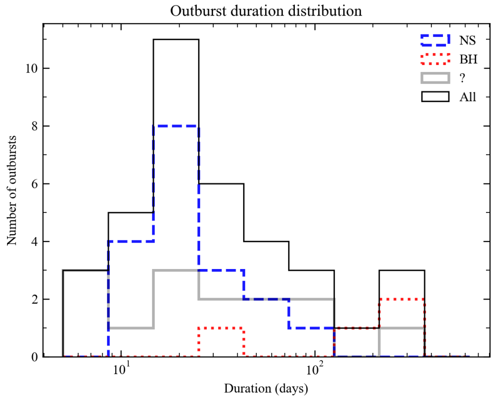

Fig. 7: Distribution of the outburst duration.

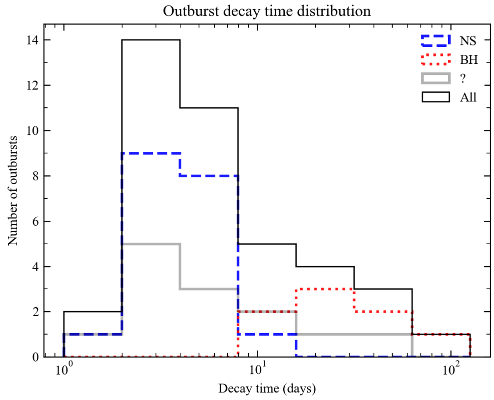

Fig. 8: Distribution of the outburst decay time.

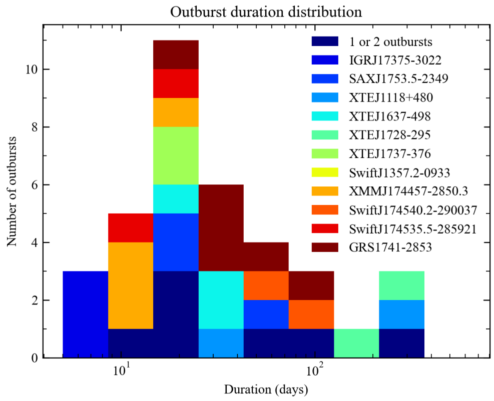

Fig. 9: Distribution of the outburst duration specified for source with more than 2 outbursts.

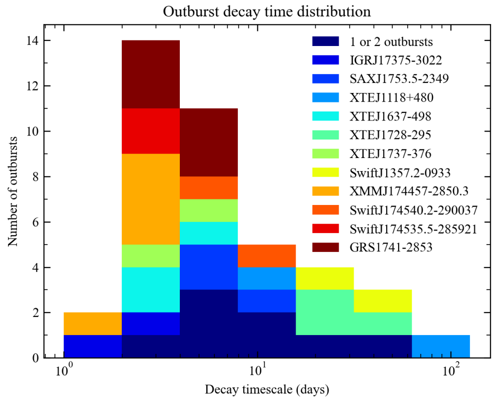

Fig. 10: Distribution of the outburst decay time for specified for source with more than 2 outbursts.

1 Source	2 BH/NS	3 Telescope	4 t_{peak} (MJD)	5 τ_{dur} r (days)	6 τ_{dec} (days)	7 Notes
XTE J1734-234	?	RXTE	51403	18.48	10.54	
IGR J17375-3022	?	RXTE	52466	5.940	0.01	
		RXTE	54750	7.380	2.41	
		RXTE	55043	7.440	1.89	
IGR J17597-2201	NS (2005)	RXTE	-	-	-	QP
		Swift	-	-	-	
SAX J1753.5-2349	NS (1999)	RXTE	51392	17.70	4.43	
		RXTE	54753	20.22	5.99	
		RXTE	55276	55.50	12.76	
WGA J1715.3-2635	?	RXTE	52501	113.72	26.86	
XTE J1118+480	BH (2001)	RXTE	51549	37.80	12.37	
		RXTE	51693	321.51	76.31	
XTE J1637-498	?	RXTE	53215	17.70	2.73	
		RXTE	53818	29.90	3.28	
		RXTE	54707	30.20	5.67	
XTE J1719-291	cNS (2011; 2015)	RXTE	54547	20.94	4.47	
XTE J1719-356	cNS (2015)	RXTE	55376	-	-	U
==XMMSL1 J171900.4-353217 (2010)		Swift	55379	-	-	U
XTE J1728-295	cBH (2011)	RXTE	52927	261.45	22.21	
		RXTE	55440	135.62	59.77	
		Swift	58584	-	30.58	
XTE J1737-376	NS (2010; 2018)	RXTE	53053	15.33	3.05	
		RXTE	54714	21.09	7.09	
XTE J1744-230	?	RXTE	-	-	-	QP
IGR J1817-155	?	RXTE	54354	61.23	7.90	
IGR J17177-3656	cBH (2011)	Swift	55635	-	11.26	
IGR J17451-3022	?	Swift	57056	-	-	HV
IGR J17494-3030	NS (2013; 2020)	Swift	56010	24.81	4.31	
SAX J1828.5-1037	NS (2002)	Swift	55875	-	-	U
Swift J1357.2-0933	BH (2013; 2015)	Swift	55595	-	30.74	
		Swift	57868	-	35.86	
XMMJ174457-2850.3	NS (2014)	Swift	54644	-	2.53	GC
		Swift	55103	12.96	1.47	
		Swift	55408	10.09	2.24	
		Swift	56153	16.06	2.48	
		Swift	57659	13.89	2.77	
Swift J174553.7-290347	?	Swift	53894	12.31	3.66	GC
Swift J174540.7-290015	?	Swift	57460	242.94	36.75	GC
Swift J174540.2-290037	?	Swift	57556	46.17	7.86	GC
		Swift		107.05	12.15	
Swift J174540.2-285921	?	Swift	55746	14.40	3.16	
		Swift	57578	16.61	2.93	
GRS 1741-2853	NS (1999; 2020)	Swift	54174	53.09	3.20	GC
		Swift	55112	40.76	5.02	
		Swift	55462	76.20	4.71	
		Swift	56517	33.19	2.21	
		Swift	57485	34.41	3.20	
		Swift	58045	24.39	7.77	

Tab. 1: All sources with their identified outbursts. For each source the type of compact object BH, candidate black hole (cBH), NS, candidate neutron star (cNS) or unknown is specified. For each outburst we noted from which telescope the observation data originates, the time at the peak of the outburst, the outburst duration, the outburst decay time and possible notifications. Notes dictionary; QP: Quasi persistant outburst, U: Unclear outburst shape due to few data points which make it unsuitable for fitting, GC: sources in the galactic center and HV: High variability in the outburst light curve resulting in a unclear decay shape.

5.4 Decay model

Table 5.4 lists all decay parameters from outbursts fitted with the decay model. The following subsections will explain the results for each source.

1 Source	2 F_t $(c\ s^{-1})$	3 F_e $(c\ s^{-1})$	4 τ_e (days)	5 τ_l (days)	6 t_t (MJD)
SAX J1753.5-2349	32.43±0.05	30.48±0.05	6.00±0.56	7.95±0.57	55298.3±1.1
XTE J1118+480	2.29*	2.13±0.01	3.38±0.71	18.45±1.35	51556.3±0.8
XTE J1118+480	2.29±0.01	2.28±0.01	15.80±6.36	30.74±4.68	51727.0±3.1
XTE J1737-376	20.85±0.03	10.09±0.08	6.12±0.33	1.94 ±0.53	54728.4±0.5
XTE J1728-295	$4.57\ 10^{-11} \pm 0.01 **$	$2.01\ 10^{-11} \pm 0.03 **$	20.22±0.69	92.05 ±1.85	58629.3±1.4
IGR J17177-3656	$1.65\ 10^{-1} \pm 0.04$	$6.86\ 10^{-2} \pm 0.05$	10.86±0.25	15.88±1.38	55662.1±1.4
XMM J174457-2850.3	$3.27\ 10^{-2} \pm 0.12$	$1.71\ 10^{-2} \pm 0.16$	2.24±0.24	3.98±0.83	54651.3±0.8

Tab. 2: Listing all decay parameters from outbursts fitted with the decay model: transition count rate F_t, exponential amplitude F_e, exponential decay time τ_e, linear decay time τ_l and the transition time t_t. The first four outburst cover data from *RXTE* and the remaining three outbursts are from *Swift*. * This value is fixed to the value of the second outburst of XTE J1118+480 (see subsection 5.4 for more detail). ** Values are not in c s^{-1} but in un absorbed flux. The errors in column 2 and 3 are relative errors.

SAX J1753.5-2349

We fitted *RXTE* data of SAX J1753.5-2349 from an outburst at MJD 55276 (March 2010) shown in figure 11. Despite the linear part of the fit is driven by only two data points the decay model provides a good approximation of the decay shape. With this fit the exponential decay time is determined at 6.00±0.56 days. Equation 9 gives a disc radius of 2.52×10^{10} cm. This source is known as a NS binary by observations of thermonuclear bursts so we assumed that $q = 0.1$ (Chakrabarty et al. 2011). This disc radius together with the mass ratio gives a orbital period of 3.66±0.34 h via equation 10.

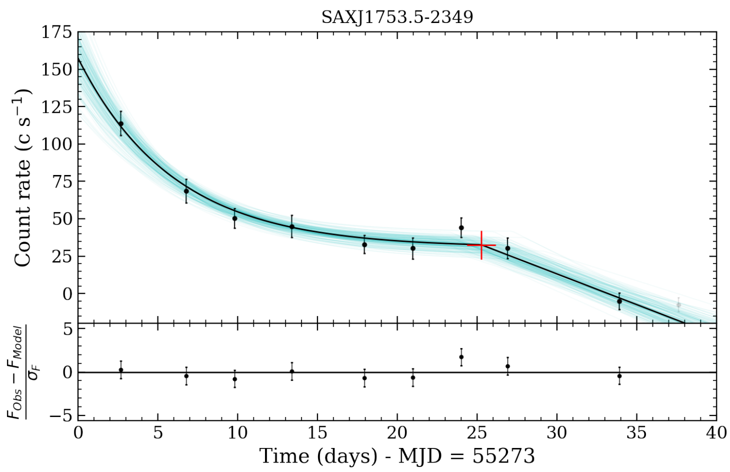

Fig. 11: Decay model fit of SAX J1753.5-2349.

XTE J1118+480

There are two outbursts visible in the *RXTE* light curve from XTE J1118+480. We first fitted the light curve from the outburst at MJD 51693 (May 2000) shown in figure 12. The decay fit seems to give a good approximation of the clearly visible transition plateau around 3 c s^{-1}. With this fit the exponential decay time is determined at 15.80±0.71 days. This gives a disc radius of 4.09×10^{10} cm by equation 9. This source is known to have a BH and a mass fraction of 0.037±0.007 (Orosz 2001; Wagner et al. 2001). This disc radius together with a mass fraction 0.037±0.007 gives a orbital period of 3.4±0.7 h via equation 10.

We checked the transition count rate from the outburst at MJD 51693 (May 2000) by fitting the outburst at MJD 51549 (May 2000) while fixing F_t to the value of the MJD 51693 (May 2000) outburst. This fit is shown in figure 13 and it seems a reasonable description indicating the transition luminosity is the same in both outbursts.

To validate the decay model we have calculated the distance using equation 11. With *PIMMS* we found a count rate to flux conversion factor of 2.852×10^{-10} ergs cm^{-2} s^{-1}. Based on the transition flux F_t this source should be at a distance of 3.08±0.04 kpc with $N_h = 0.99\times10^{22}$ as in Stoop et al. 2021.

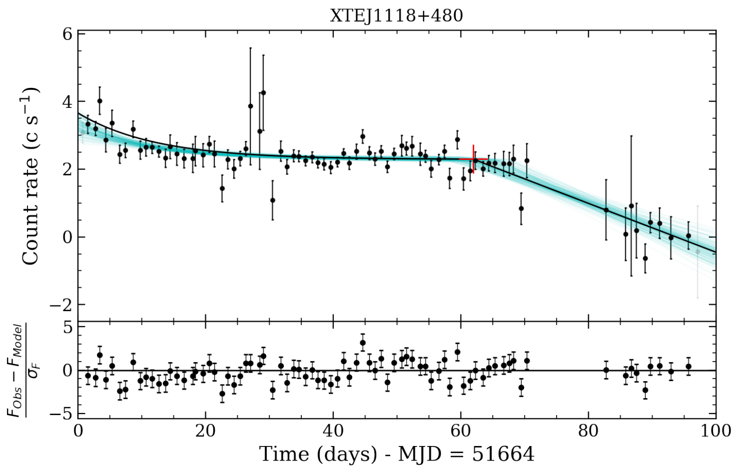

Fig. 12: Decay model fit of XTE J1118+480.

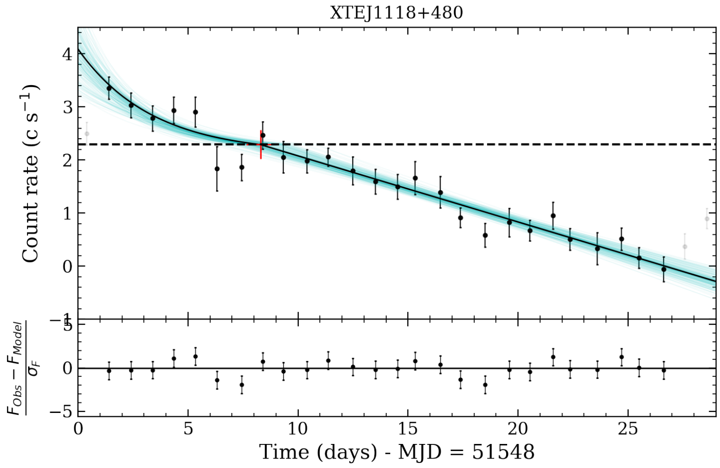

Fig. 13: Decay model fit of XTE J1118+480.

XTE J1737-376

We fitted *RXTE* data of XTE J1737-376 (==IGR J17379–3747) from an outburst at MJD 54714 (September 2008) shown in figure 14. The linear part of the decay model is driven by only two data points however the decay model gives a more accurate description of the exponential part. With this fit the exponential decay time is determined at 6.12±0.33 days. Equation 9 gives a disc radius of 2.55×10^{10} cm. This source is known as a NS binary by observations of X-ray pulsations (Sanna et al. 2018). The same study obtained a mass fraction that $q = 0.04$. The disc radius together with a mass ratio of $q = 0.04$ (Sanna et al. 2018) gives a orbital period of 2.05±0.10 h via equation 10.

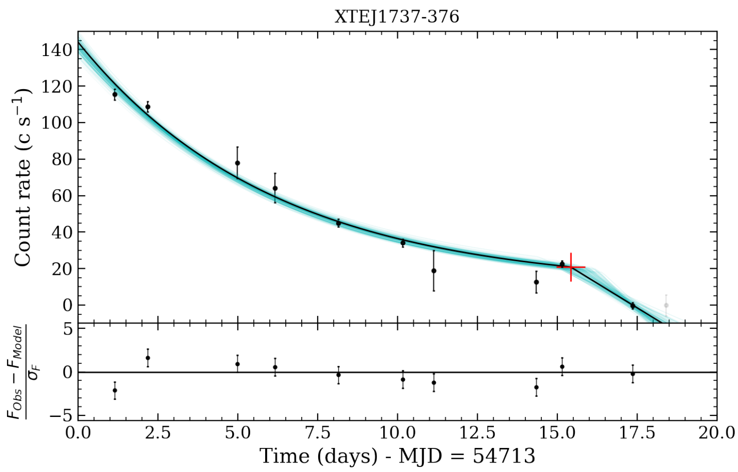

Fig. 14: Decay model fit of XTE J1737-376.

XTE J1728-295

We fitted *Swift* data of XTE J1728-295 (==IGR J17285-2922) from an outburst at MJD 58584 (April 2019) shown in figure 15. The decay model seems to provide an accurate description of the whole decay shape since the exponential and linear part contain sufficient number of data points. With this fit the exponential decay time is determined at 20.22±0.69 days. Equation 9 gives a disc radius of 4.63×10^{10} cm. From spectral analysis there are indications for this source to be a BH binary (Sidoli et al. 2011; Stoop et al. 2021). The disc radius together with a mass ratio of $q = 0.01$ (Stoop et al. 2021) gives a orbital period of 2.17±0.05 h via equation 10.

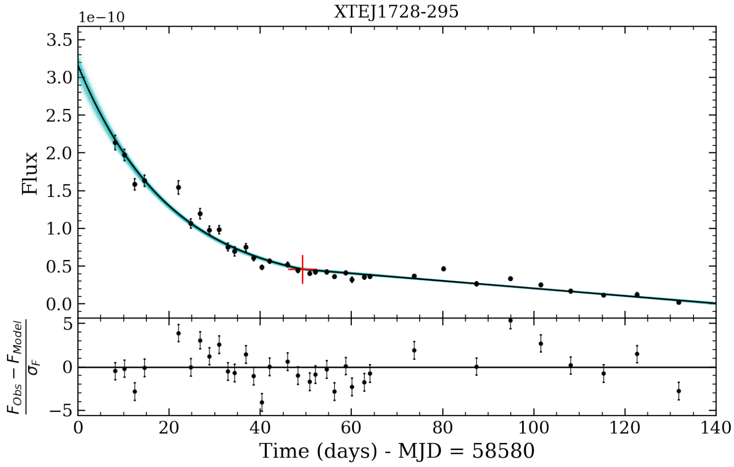

Fig. 15: Decay model fit of XTE J1728-295.

IGR J17177-3656

We fitted *Swift* data of IGR J17177-3656 from an outburst at MJD 55635 (March 2011) shown in figure 16. Although the transition from exponential to linear is not as clear as in XTE J1118+480 the decay model seems to provide a good description of the decay shape. With this fit the exponential decay time is determined at 6.12±0.33 days. This source is thought to be a BH binary by observations in X-ray and radio (Paizis et al. 2011). Equation 9 gives a disc radius of 3.39×10^{10} cm. The disc radius together with a assumed mass ratio of $q = 0.1$ gives a orbital period of 5.70±0.13 h via equation 10.

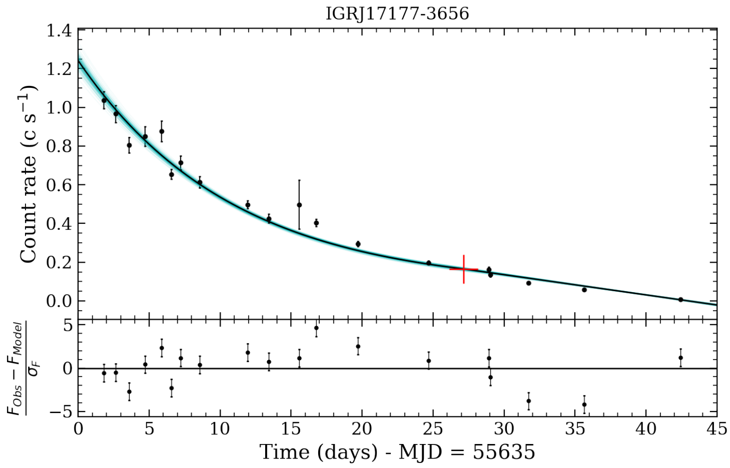

Fig. 16: Decay model fit of IGR J17177-3656.

XMMJ174457-2850.3

We fitted *Swift* data of XMMJ174457-2850.3 from an outburst at MJD 54644 (June 2008) shown in figure 17. Despite the low number of data points (three in the exponential part and four in the linear part) the relatively small errors on the light curve indicate that this fit gives a reasonable description of the decay shape. With this fit the exponential decay time is determined at 2.24$\pm$0.24 days. This source is thought to be a NS binary by observations of thermonuclear bursts (Degenaar et al. 2012). Equation 9 gives a disc radius of 1.54×10^{10} cm. The disc radius together with a assumed mass ratio of $q = 0.1$ gives a orbital period of 1.81$\pm$0.12 h via equation 10 as in Heinke et al. 2015.

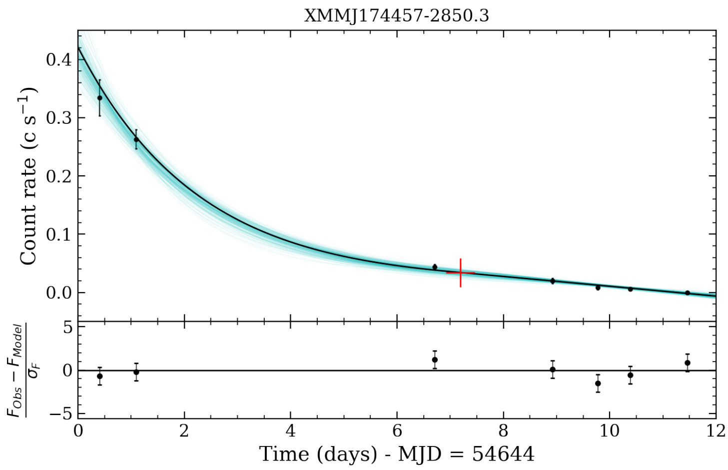

Fig. 17: Decay model fit of XMMJ174457-2850.3.

6 Discussion

This work presents the first systematic analysis of outburst light curves from 21 VFXBs. We first characterized the typical outburst duration and decay time. We then fitted an accretion disc model on well-sampled light curves to extract the orbital periods, which resulted in short orbital periods of 2 to 6 hours on 6 sources. The following subsections will discuss the implications of our results.

6.1 Typical duration and decay time

The duration and decay time distribution shows a similar general shape to that of bright sources (Yan and Yu 2015). However, the duration and decay time seems to be skewed to lower values compared to bright sources (Yan and Yu 2015). This might indicate the VFXBs have smaller accretion disc and therefore shorter orbital periods (Wu et al. 2010). Our results show that BHs seems to have longer outbursts and decay times. Most BHs we observe are having large accretion discs (Tetarenko et al. 2016) and therefore longer outbursts and decay times which explains the difference between NSs and BHs in the duration and decay time distributions (Wu et al. 2010). This gives indications for a similar accretion process in both bright and very faint sources although the number statistics for the latter group is still very modest. The distributions in figure 9 and 10 illustrates the effect of limited number of sources. Most sources contain more than 2 outbursts and therefore have a larger impact on the final distribution shape in figure 7 and 8. For example GRS 1741-2853 is dominating a significant part in both distributions.

We note that Yan and Yu 2015 used other methods to determine the duration and decay time. In their method they select data points above a certain percentage from the peak rate. We have tested their method on WGAJ1715.3-2635 and found a duration more than 6 times larger than our selected outburst region. Because most light curves from VFXBs have low count rates and therefore higher noise levels this method turned out to be not useful for our light curves.

6.2 Orbital periods

For all six sources that had sufficiently well sampled light curves to fit the decay model we have found short orbital periods of 1.8 h to 5.7 h which matches with the expectation from Wu et al. 2010. On two sources we were able to validate the model using independent observations. For XTE J1118+480 we obtained a distance of 3.07 ± 0.03 kpc which is matching with observations ranging from 3 to 8 kpc (Gandhi et al. 2019). For XTE J1737-376 we found a orbital period of 2.05 ± 0.10 h which matches with $\sim$1.9h determined from timing analysis of its X-ray pulsations (Sanna et al. 2018). This gives indications that the accretion disc model can be applied on VFXBs that show a clear transition and is useful to obtain an estimate of their orbital period.

Most outbursts do not contain enough data points which makes the identification of a transition from exponential to linear decay difficult. Also in most light curves of VFXBs count rates are low and therefore hard to conclude if the model is working better than a complete linear or exponential for example. But for 7 outbursts the results look promising combined with the fact that observations match on 2 sources giving strong indications the decay model works. Therefore it is interesting to use and test the validity of this model further on future outbursts. For this to work we recommend future outburst observations with a 1 - 3 days observation interval all the way to quiescence.

7 Conclusion

We have performed a first systematic study of outburst light curves from 21 VFXBs. Similar trends as in bright X-ray binaries in the distribution for the duration and decay time were found. BHs seem to have longer outbursts and decay times explained by the larger accretion discs of BHs (Wu et al. 2010) indicating a accretion process similar to bright sources. Using the accretion disc model we have found orbital periods of 2 to 6 hours supporting evidence that VFXBs have shorter orbital periods. For XTE J1118+480 and XTE J1737-376 the accretion disc model predicts an orbital period and distance matching with independent observations. So far the number of observations is the most limiting factor to fit the accretion disc model. Therefore more outburst showing enough data points to identify a transition are needed to test the instability model at a more convincingly way.

References

M. Armas Padilla, N. Degenaar, R. Kaur, R. Wijnands, and Y. Yang. XMMSL1 J171900.4-353217 returns to quiescence. *The Astronomer's Telegram*, 2738:1, July 2010.

M. Armas Padilla, N. Degenaar, A. Patruno, D. M. Russell, M. Linares, T. J. Maccarone, J. Homan, and R. Wijnands. X-ray softening in the new X-ray transient XTE J1719291 during its 2008 outburst decay. *Monthly Notices of the Royal Astronomical Society*, 417(1):659–665, 10 2011. ISSN 0035-8711. doi: 10.1111/j.1365-2966.2011.19308.x. URL https://doi.org/10.1111/j.1365-2966.2011.19308.x.

M. Armas Padilla, R. Wijnands, and N. Degenaar. XMM–Newton and Swift spectroscopy of the newly discovered very faint X-ray transient IGR J17494–3030. *Monthly Notices of the Royal Astronomical Society: Letters*, 436(1):L89–L93, 09 2013. ISSN 1745-3925. doi: 10.1093/mnrasl/slt119. URL https://doi.org/10.1093/mnrasl/slt119.

Astropy Collaboration and Thomas P. Robitaille. Astropy: A community Python package for astronomy. , 558:A33, October 2013. doi: 10.1051/0004-6361/201322068. URL https://ui.adsabs.harvard.edu/abs/2013A&A...558A..33A.

Luca Baiotti, Bruno Giacomazzo, and Luciano Rezzolla. Accurate evolutions of inspiralling neutron-star binaries: Prompt and delayed collapse to a black hole. *Phys. Rev. D*, 78:084033, Oct 2008. doi: 10.1103/PhysRevD.78.084033. URL https://link.aps.org/doi/10.1103/PhysRevD.78.084033.

Deepto Chakrabarty, Peter Jonker, and Craig B. Markwardt. Chandra Localization of SAX J1806.5-2215. *The Astronomer's Telegram*, 3218:1, March 2011. URL https://ui.adsabs.harvard.edu/abs/2011ATel.3218....1C.

I. V. Chelovekov and S. A. Grebenev. Investigation of the transient X-ray burster IGR J17380-3749 discovered by the INTEGRAL observatory. *Astronomy Letters*, 36(12):895–903, December 2010. doi: 10.1134/S1063773710120030.

Wan Chen, C. R. Shrader, and Mario Livio. The Properties of X-Ray and Optical Light Curves of X-Ray Novae. , 491(1):312–338, December 1997. doi: 10.1086/304921. URL https://ui.adsabs.harvard.edu/abs/1997ApJ...491..312C.

M. Cocchi, A. Bazzano, L. Natalucci, P. Ubertini, J. Heise, J. M. Muller, and J. J. M. in 't Zand. Discovery of type-I X-ray bursts from GRS 1741.9-2853. , 346:L45–L48, June 1999. URL https://ui.adsabs.harvard.edu/abs/1999A&A...346L..45C.

R. Cornelisse, F. Verbunt, J. J. M. in't Zand, E. Kuulkers, J. Heise, R. A. Remillard, M. Cocchi, L. Natalucci, A. Bazzano, and P. Ubertini. BeppoSAX Wide Field Cameras observations of six type I X-ray bursters. , 392:885–893, September 2002. doi: 10.1051/0004-6361:20020707. URL https://ui.adsabs.harvard.edu/abs/2002A&A...392..885C.

J. M. Corral-Santana, J. Casares, T. Muñoz-Darias, P. Rodríguez-Gil, T. Shahbaz, M. A. P. Torres, C. Zurita, and A. A. Tyndall. A Black Hole Nova Obscured by an Inner Disk Torus. *Science*, 339(6123):1048–1051, March 2013. doi: 10.1126/science.1228222. URL https://ui.adsabs.harvard.edu/abs/2013Sci...339.1048C.

J. M. Corral-Santana, J. Casares, T. Muñoz-Darias, F. E. Bauer, I. G. Martínez-Pais, and D. M. Russell. Blackcat: A catalogue of stellar-mass black holes in x-ray transients. *Astronomy Astrophysics*, 587: A61, Feb 2016. ISSN 1432-0746. doi: 10.1051/0004-6361/201527130. URL http://dx.doi.org/10.1051/0004-6361/201527130.

N. Degenaar and R. Wijnands. The behavior of subluminous X-ray transients near the Galactic center as observed using the X-ray telescope aboard Swift. , 495(2):547–559, February 2009. doi: 10.1051/0004-6361:200810654. URL https://ui.adsabs.harvard.edu/abs/2009A&A...495..547D.

N. Degenaar, J. A. Kennea, R. Wijnands, J. M. Miller, and N. Gehrels. The galactic center X-ray transient XMM J174457-2850.3 is a neutron star low-mass X-ray binary. *The Astronomer's Telegram*, 4308:1, August 2012. URL https://ui.adsabs.harvard.edu/abs/2012ATel.4308....1D.

N. Degenaar, R. Wijnands, M. T. Reynolds, J. M. Miller, D. Altamirano, J. Kennea, N. Gehrels, D. Haggard, and G. Ponti. THE PECULIAR GALACTIC CENTER NEUTRON STAR x-RAY BINARY XMM j174457-2850.3. *The Astrophysical Journal*, 792(2):109, aug 2014. doi: 10.1088/0004-637x/792/2/109. URL https://doi.org/10.1088/0004-637x/792/2/109.

N. Degenaar, R. Wijnands, J. M. Miller, M. T. Reynolds, J. Kennea, and N. Gehrels. The Swift X-ray monitoring campaign of the center of the Milky Way. *Journal of High Energy Astrophysics*, 7:137–147, September 2015. doi: 10.1016/j.jheap.2015.03.005. URL https://ui.adsabs.harvard.edu/abs/2015JHEAp...7..137D.

N. Degenaar, R. Wijnands, M. T. Reynolds, J. M. Miller, and J. A. Kennea. Swift/XRT detects a new outburst of the Galactic Center transient GRS 1741.9-2853. *The Astronomer's Telegram*, 13683:1, April 2020. URL https://ui.adsabs.harvard.edu/abs/2020ATel13683....1D.

P. A. Evans, A. P. Beardmore, K. L. Page, L. G. Tyler, J. P. Osborne, M. R. Goad, P. T. O'Brien, L. Vetere, J. Racusin, D. Morris, D. N. Burrows, M. Capalbi, M. Perri, N. Gehrels, and P. Romano. An online repository of Swift/XRT light curves of γ-ray bursts. , 469(1):379–385, July 2007. doi: 10.1051/0004-6361:20077530. URL https://ui.adsabs.harvard.edu/abs/2007A&A...469..379E.

Juhan Frank, Andrew King, and Derek J. Raine. *Accretion Power in Astrophysics: Third Edition*. 2002. URL https://ui.adsabs.harvard.edu/abs/2002apa..book.....F.

Poshak Gandhi, Anjali Rao, Michael A. C. Johnson, John A. Paice, and Thomas J. Maccarone. Gaia Data Release 2 distances and peculiar velocities for Galactic black hole transients. , 485(2):2642–2655, May 2019. doi: 10.1093/mnras/stz438. URL https://ui.adsabs.harvard.edu/abs/2019MNRAS.485.2642G.

J.-M. Hameury and J.-P. Lasota. Outbursts in ultracompact x-ray binaries. *Astronomy Astrophysics*, 594:A87, Oct 2016. ISSN 1432-0746. doi: 10.1051/0004-6361/201628434. URL http://dx.doi.org/10.1051/0004-6361/201628434.

J.M. Hameury. A review of the disc instability model for dwarf novae, soft x-ray transients and related objects. *Advances in Space Research*, 66(5):1004–1024, 2020. ISSN 0273-1177. doi: https://doi.org/10.1016/j.asr.2019.10.022. URL https://www.sciencedirect.com/science/article/pii/S0273117719307586. Nova Eruptions, Cataclysmic Variables and Related Systems: Challenges in the 2020 Era.

C. O. Heinke, A. Bahramian, N. Degenaar, and R. Wijnands. The nature of very faint X-ray binaries: hints from light curves. *Monthly Notices of the Royal Astronomical Society*, 447(4):3034–3043, 01 2015. ISSN 0035-8711. doi: 10.1093/mnras/stu2652. URL https://doi.org/10.1093/mnras/stu2652.

Craig O. Heinke, Haldan N. Cohn, and Phyllis M. Lugger. THE DISCOVERY OF a VERY FAINT x-RAY TRANSIENT IN THE GLOBULAR CLUSTER m15. *The Astrophysical Journal*, 692 (1):584–593, feb 2009. doi: 10.1088/0004-637x/692/1/584. URL https://doi.org/10.1088/0004-637x/692/1/584.

in 't Zand, J. J. M., Jonker, P. G., and Markwardt, C. B. Six new candidate ultracompact x-ray binaries. *A&A*, 465(3):953–963, 2007. doi: 10.1051/0004-6361:20066678. URL https://doi.org/10.1051/0004-6361:20066678.

J. J. M. In't Zand, J. Heise, J. M. Muller, A. Bazzano, M. Cocchi, L. Natalucci, and P. Ubertini. Discovery of SAX J1753.5-2349 and SAX J1806.5-2215: two X-ray bursters without detectable steady emission. *Nuclear Physics B Proceedings Supplements*, 69(1-3):228–231, January 1999. doi: 10.1016/S0920-5632(98)00214-X. URL https://ui.adsabs.harvard.edu/abs/1999NuPhS..69..228I.

A. R. King and R. Wijnands. The faintest accretors. *Monthly Notices of the Royal Astronomical Society: Letters*, 366(1):L31–L34, 02 2006. ISSN 1745-3925. doi: 10.1111/j.1745-3933.2005.00126.x. URL https://doi.org/10.1111/j.1745-3933.2005.00126.x.

A.R. King and H. Ritter. The light curves of soft X-ray transients. *Monthly Notices of the Royal Astronomical Society*, 293(1):L42–L48, 01 1998. ISSN 0035-8711. doi: 10.1046/j.1365-8711.1998.01295.x. URL https://doi.org/10.1046/j.1365-8711.1998.01295.x.

Jean-Pierre Lasota. The disc instability model of dwarf novae and low-mass X-ray binary transients. , 45(7):449–508, June 2001. doi: 10.1016/S1387-6473(01)00112-9. URL https://ui.adsabs.harvard.edu/abs/2001NewAR..45..449L.

Q. Z. Liu, J. van Paradijs, and E. P. J. van den Heuvel. A catalogue of low-mass X-ray binaries in the Galaxy, LMC, and SMC (Fourth edition). , 469(2):807–810, July 2007. doi: 10.1051/0004-6361:20077303. URL https://ui.adsabs.harvard.edu/abs/2007A&A...469..807L.

A. Lutovinov, M. Revnivtsev, S. Molkov, and R. Sunyaev. INTEGRAL observations of five sources in the Galactic Center region. , 430:997–1003, February 2005. doi: 10.1051/0004-6361:20041677. URL https://ui.adsabs.harvard.edu/abs/2005A&A...430..997L.

C. Markwardt, T. Strohmayer, and J. Swank. Xmmsl1 j171900.4-353217 and xte j1719-356 are probably the same source. *The Astronomer's Telegram*, 05 2010.

D. Mata Sánchez, T. Muñoz-Darias, J. Casares, J. M. Corral-Santana, and T. Shahbaz. Swift J1357.2-0933: a massive black hole in the Galactic thick disc. , 454(2):2199–2204, December 2015. doi: 10.1093/mnras/stv2111.

K. Mukai. PIMMS tool. *Legacy*, 3:21–31, October 1993.

M. P. Muno, J. R. Lu, F. K. Baganoff, W. N. Brandt, G. P. Garmire, A. M. Ghez, S. D. Hornstein, and M. R. Morris. A remarkable low-mass x-ray binary within 0.1 parsecs of the galactic center. *The*

Astrophysical Journal, 633(1):228–239, nov 2005. doi: 10.1086/444586. URL https://doi.org/10.1086/444586.

Mason Ng, Paul S. Ray, Peter Bult, Deepto Chakrabarty, Gaurava K. Jaisawal, Christian Malacaria, Diego Altamirano, Zaven Arzoumanian, Keith C. Gendreau, Tolga Güver, Matthew Kerr, Tod E. Strohmayer, Zorawar Wadiasingh, and Michael T. Wolff. NICER Discovery of Millisecond X-Ray Pulsations and an Ultracompact Orbit in IGR J17494-3030. , 908(1):L15, February 2021. doi: 10.3847/2041-8213/abe1b4. URL https://ui.adsabs.harvard.edu/abs/2021ApJ...908L..15N.

A. T. Okazaki and I. Negueruela. A natural explanation for periodic X-ray outbursts in Be/X-ray binaries. , 377:161–174, October 2001. doi: 10.1051/0004-6361:20011083. URL https://ui.adsabs.harvard.edu/abs/2001A&A...377..161O.

Jerome Orosz. The spectroscopic mass ratio of the black hole binary xte j1118+480. *The Astronomer's Telegram*, pages 1–, 05 2001.

A. Paizis, M. A. Nowak, J. Wilms, S. Chaty, S. Corbel, J. Rodriguez, M. Del Santo, P. Ubertini, and R. Chini. Unveiling the Nature of IGR J17177-3656 with X-Ray, Near-infrared, and Radio Observations. , 738(2):183, September 2011. doi: 10.1088/0004-637X/738/2/183. URL https://ui.adsabs.harvard.edu/abs/2011ApJ...738..183P.

Craig R. Powell, Carole A. Haswell, and Maurizio Falanga. Mass transfer during low-mass X-ray transient decays. , 374(2):466–476, January 2007. doi: 10.1111/j.1365-2966.2006.11144.x. URL https://ui.adsabs.harvard.edu/abs/2007MNRAS.374..466P.

A. Sanna, E. Bozzo, A. Papitto, A. Riggio, C. Ferrigno, T. Di Salvo, R. Iaria, S. M. Mazzola, N. D'Amico, and L. Burderi. Xmm-newton detection of the 2.1 ms coherent pulsations from igr j17379–3747. *Astronomy Astrophysics*, 616:L17, Aug 2018. ISSN 1432-0746. doi: 10.1051/0004-6361/201833205. URL http://dx.doi.org/10.1051/0004-6361/201833205.

T. Shahbaz, P. A. Charles, and A. R. King. Soft X-ray transient light curves as standard candles: exponential versus linear decays. , 301(2):382–388, December 1998. doi: 10.1046/j.1365-8711.1998.01991.x. URL https://ui.adsabs.harvard.edu/abs/1998MNRAS.301..382S.

L. Sidoli, A. Paizis, S. Mereghetti, D. Götz, and M. Del Santo. XMM-Newton and INTEGRAL observations of the very faint X-ray transient IGR J17285-2922/XTE J1728-295 during the 2010 outburst. , 415(3):2373–2378, August 2011. doi: 10.1111/j.1365-2966.2011.18865.x. URL https://ui.adsabs.harvard.edu/abs/2011MNRAS.415.2373S.

Jean Swank and Craig Markwardt. Populations of Transient Galactic Bulge X-ray Sources. 251:94, January 2001. URL https://ui.adsabs.harvard.edu/abs/2001ASPC..251...94S.

B. E. Tetarenko, G. R. Sivakoff, C. O. Heinke, and J. C. Gladstone. Watchdog: A comprehensive all-sky database of galactic black hole x-ray binaries. *The Astrophysical Journal Supplement Series*, 222(2):15, Feb 2016. ISSN 1538-4365. doi: 10.3847/0067-0049/222/2/15. URL http://dx.doi.org/10.3847/0067-0049/222/2/15.

M. A. P. Torres, P. J. Callanan, M. R. Garcia, P. Zhao, S. Laycock, and A. K. H. Kong. MMT observations of the black hole candidate XTE j1118480 near and in quiescence. *The Astrophysical Journal*, 612(2):1026–1033, sep 2004. doi: 10.1086/422740. URL https://doi.org/10.1086/422740.

Derek Tournear, E. Raffauf, Elliott Bloom, W. Focke, B. Giebels, Gary Godfrey, Pablo Saz Parkinson, Kaice Reilly, K. Wood, P. Ray, M. Wolff, Reba Bandyopadhyay, Michael Lovellette, and Jeffrey Scargle. X-ray bursts in neutron star and black hole binaries from unconventional stellar aspect experiment and rossi x-ray timing explorer data: Detections and upper limits. *The Astrophysical Journal*, 595:1058, 12 2008. doi: 10.1086/377431.

J. van den Eijnden, N. Degenaar, R. Wijnands, T. D. Russell, M. Stoop, M. Armas Padilla, D. M. Russell, D. Maitra, C. O. Heinke, G. R. Sivakoff, A. W. Shaw, T. J. Maccarone, J. C. A. Miller-Jones, and A. Bahramian. VLA detection of a likely radio counterpart of IGR J17494-3030. *The Astronomer's Telegram*, 14129:1, October 2020. URL https://ui.adsabs.harvard.edu/abs/2020ATel14129....1V.

R. Mark Wagner, C. B. Foltz, T. Shahbaz, J. Casares, P. A. Charles, S. G. Starrfield, and P. Hewett. The halo black hole x-ray transient XTE j1118480. *The Astrophysical Journal*, 556(1):42–46, jul 2001. doi: 10.1086/321572. URL https://doi.org/10.1086/321572.

R. Wijnands, J. J. M. in 't Zand, M. Rupen, T. Maccarone, J. Homan, R. Cornelisse, R. Fender, J. Grindlay, M. van der Klis, E. Kuulkers, and et al. Thexmm-newton/chandramonitoring campaign of the galactic center region. *Astronomy Astrophysics*, 449(3):1117–1127, Mar 2006. ISSN 1432-0746. doi: 10.1051/0004-6361:20054129. URL http://dx.doi.org/10.1051/0004-6361:20054129.

R. Wijnands, N. Degenaar, M. Armas Padilla, D. Altamirano, Y. Cavecchi, M. Linares, A. Bahramian, and C. O. Heinke. Low-level accretion in neutron star X-ray binaries. *Monthly Notices of the Royal Astronomical Society*, 454(2):1371–1386, 10 2015. ISSN 0035-8711. doi: 10.1093/mnras/stv1974. URL https://doi.org/10.1093/mnras/stv1974.

Y. X. Wu, W. Yu, T. P. Li, T. J. Maccarone, and X. D. Li. Orbital Period and Outburst Luminosity of Transient Low Mass X-ray Binaries. , 718(2):620–631, August 2010. doi: 10.1088/0004-637X/718/2/620. URL https://ui.adsabs.harvard.edu/abs/2010ApJ...718..620W.

Zhen Yan and Wenfei Yu. X-Ray Outbursts of Low-mass X-Ray Binary Transients Observed in the RXTE Era. , 805(2):87, June 2015. doi: 10.1088/0004-637X/805/2/87. URL https://ui.adsabs.harvard.edu/abs/2015ApJ...805...87Y.

8 Apendix

8.1 Light curves

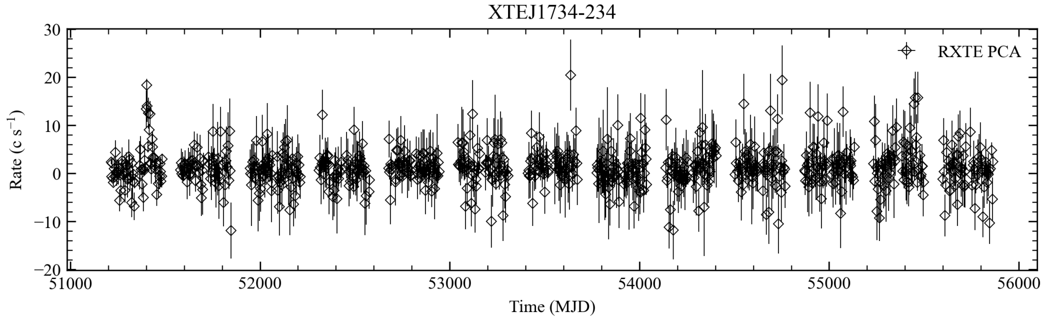

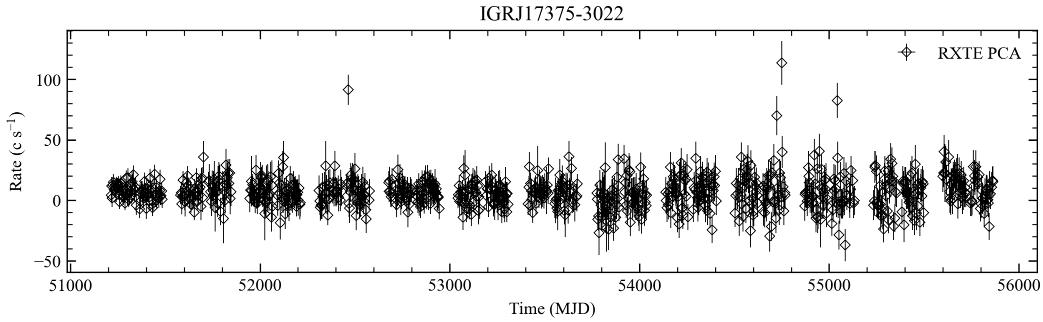

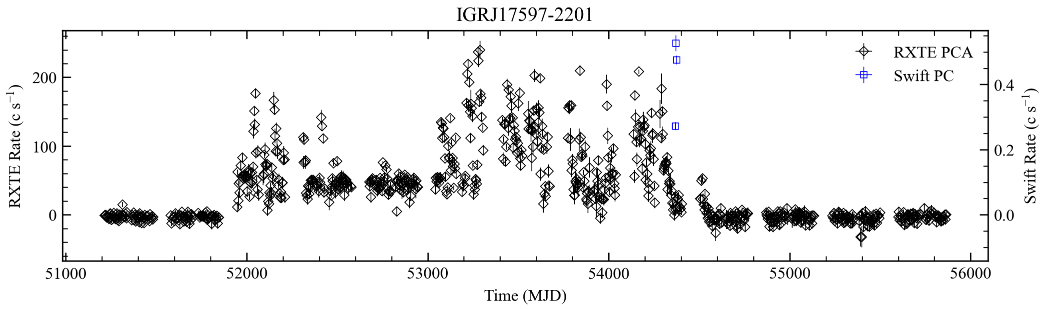

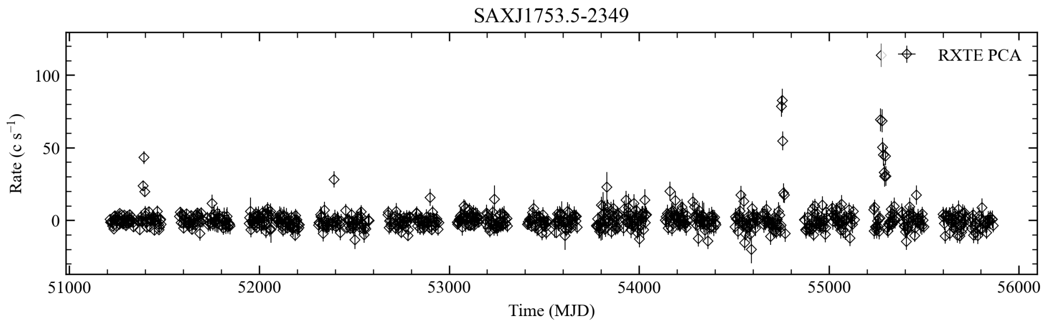

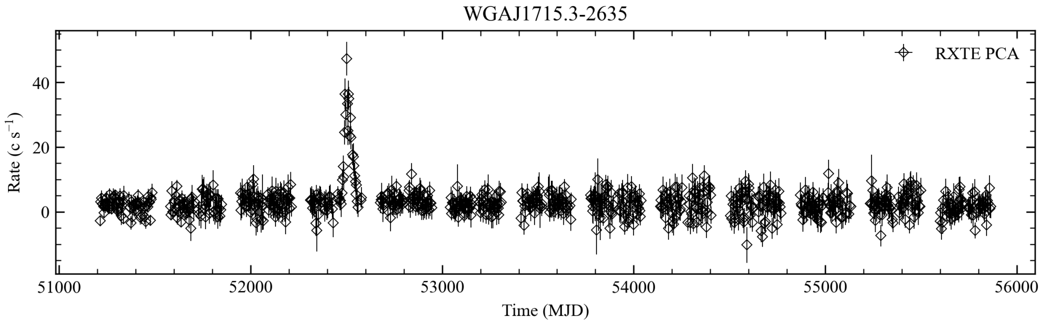
WGAJ1715.3-2635
RXTE PCA
Rate (c s^{-1})
40
20
0
51000
52000
53000
54000
55000
56000
Time (MJD)

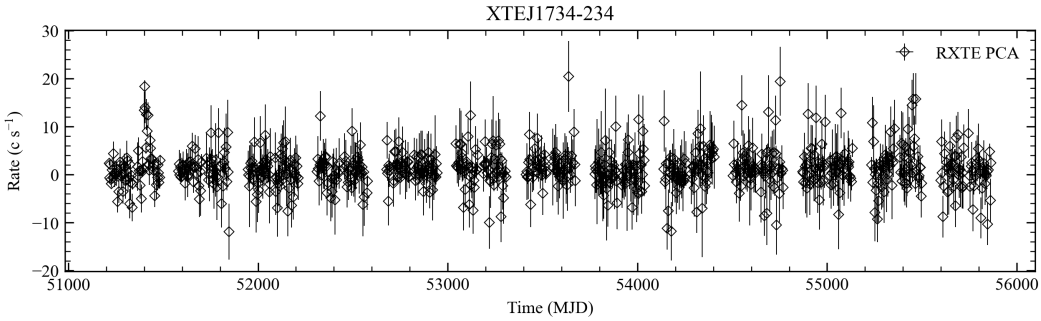
XTEJ1734-234
RXTE PCA
Rate (c s^{-1})
30
20
10
0
−10
−20
51000
52000
53000
54000
55000
56000
Time (MJD)

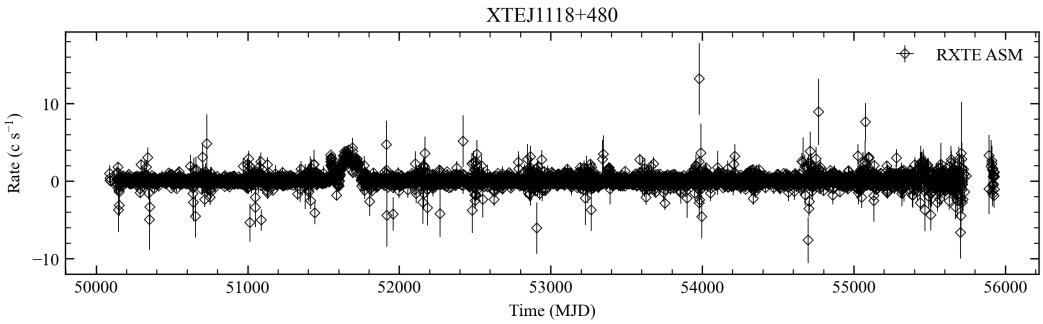
XTEJ1118+480
RXTE ASM
Rate (c s^{-1})
10
0
−10
50000
51000
52000
53000
54000
55000
56000
Time (MJD)

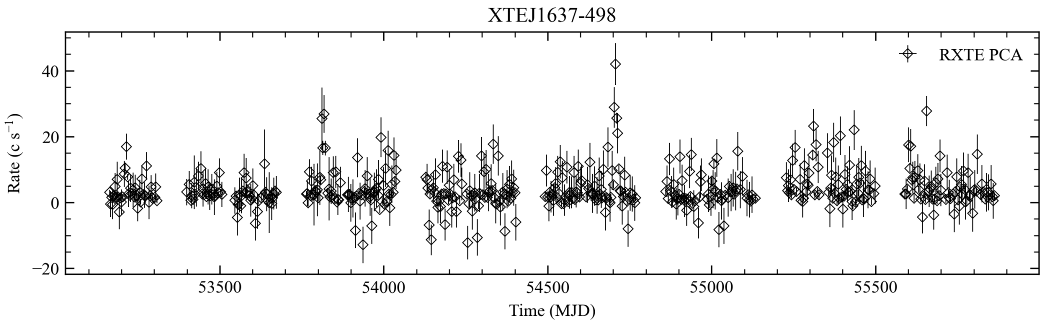
XTEJ1637-498
RXTE PCA
Rate (c s^{-1})
40
20
0
−20
53500
54000
54500
55000
55500
Time (MJD)

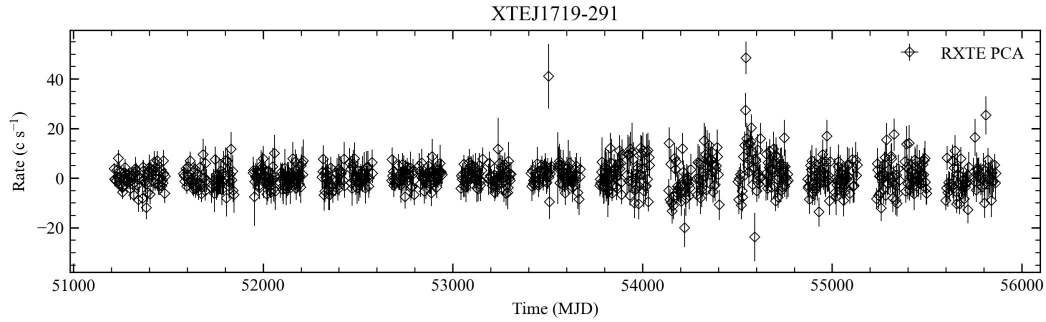
XTEJ1719-291
RXTE PCA
Rate (c s^{-1})
Time (MJD)

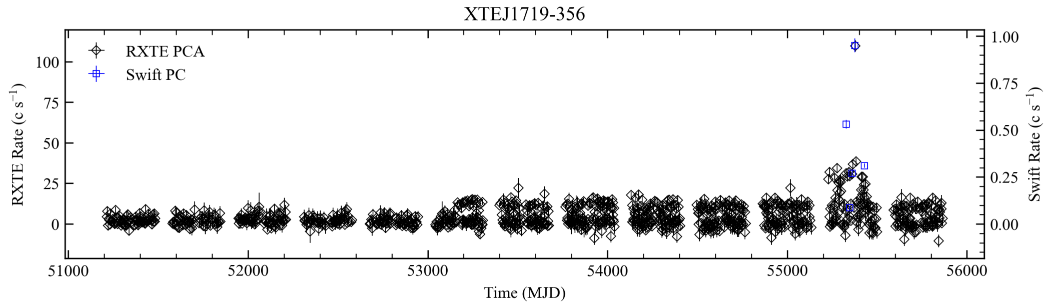
XTEJ1719-356
RXTE PCA
Swift PC
RXTE Rate (c s^{-1})
Swift Rate (c s^{-1})
Time (MJD)

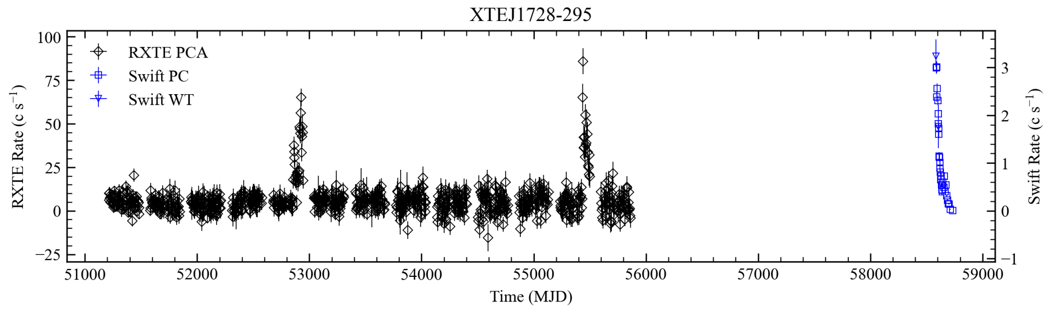
XTEJ1728-295
RXTE PCA
Swift PC
Swift WT
RXTE Rate (c s^{-1})
Swift Rate (c s^{-1})
Time (MJD)

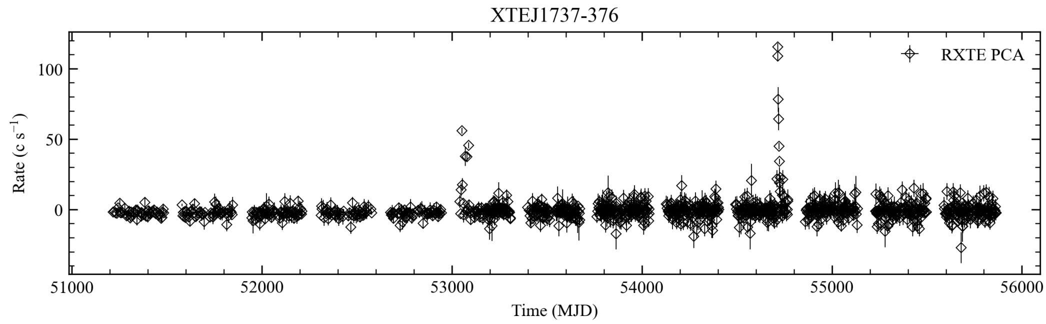
XTEJ1737-376
RXTE PCA
Rate (c s^{-1})
Time (MJD)

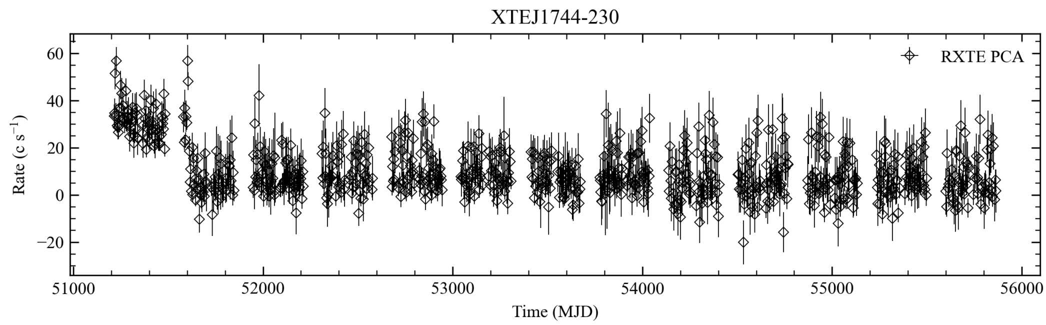
XTEJ1744-230
RXTE PCA
Rate (c s^{-1})
Time (MJD)

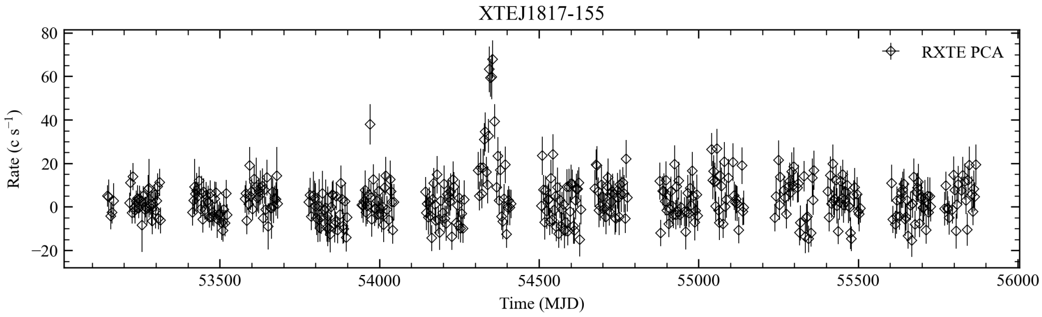
XTEJ1817-155
RXTE PCA
Rate (c s^{-1})
Time (MJD)

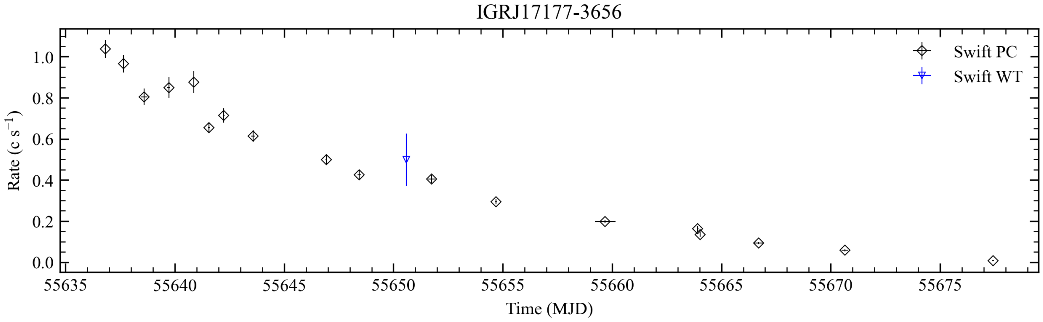
IGRJ17177-3656
Swift PC
Swift WT
Rate (c s^{-1})
Time (MJD)

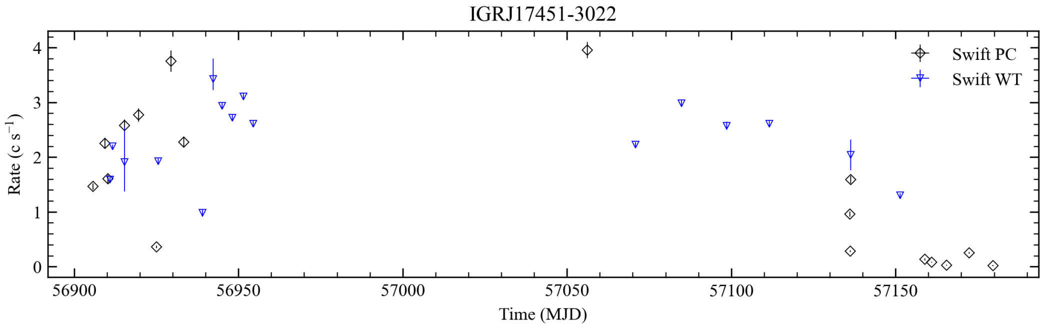
IGRJ17451-3022
Swift PC
Swift WT
Rate (c s^{-1})
Time (MJD)

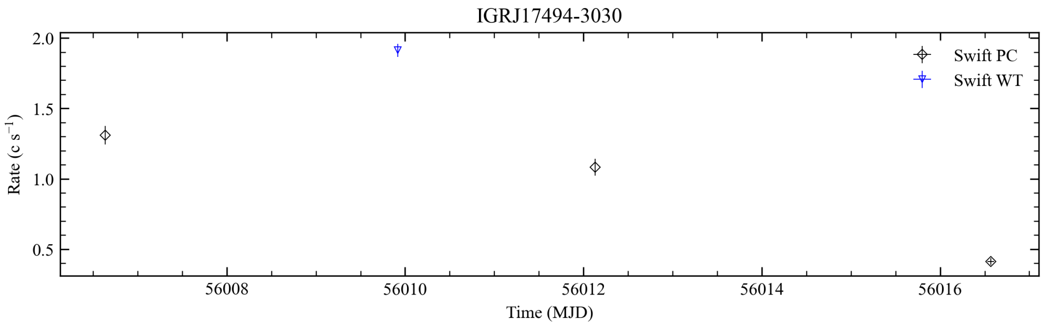
IGRJ17494-3030
Swift PC
Swift WT
Rate (c s^{-1})
Time (MJD)

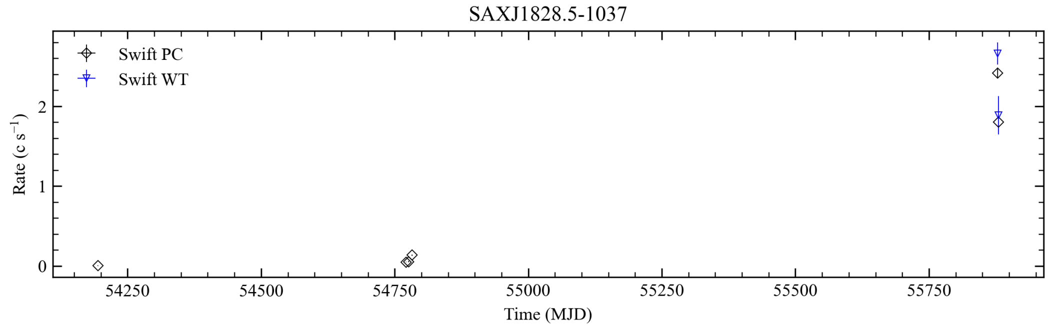
SAXJ1828.5-1037
Swift PC
Swift WT
Rate (c s^{-1})
Time (MJD)

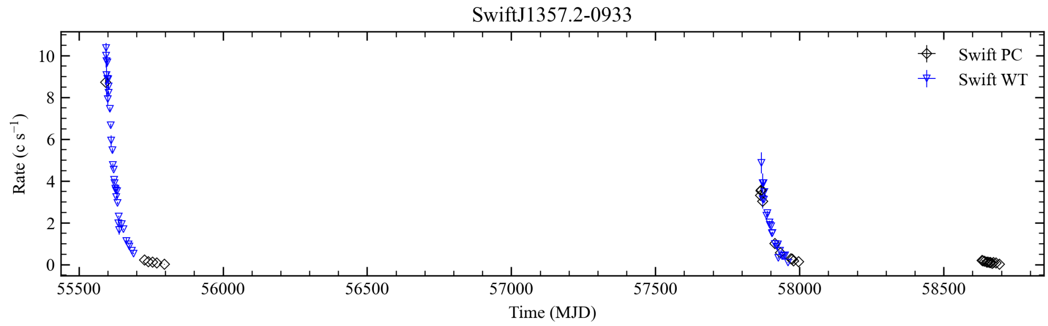
SwiftJ1357.2-0933
Swift PC
Swift WT
Rate (c s^{-1})
Time (MJD)

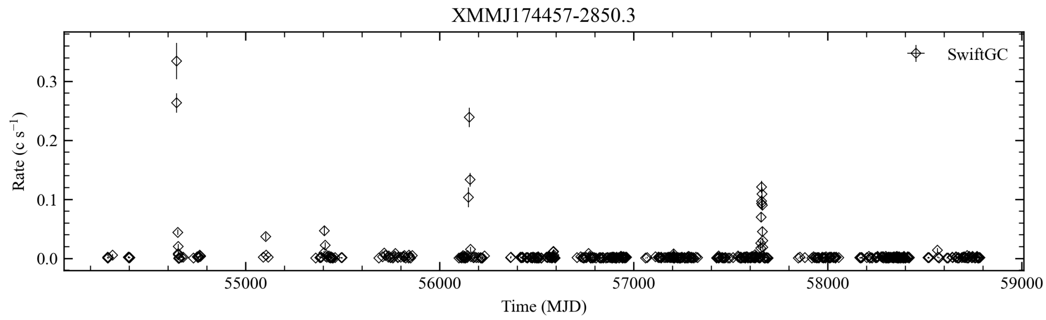
XMMJ174457-2850.3
SwiftGC
Rate (c s^{-1})
Time (MJD)

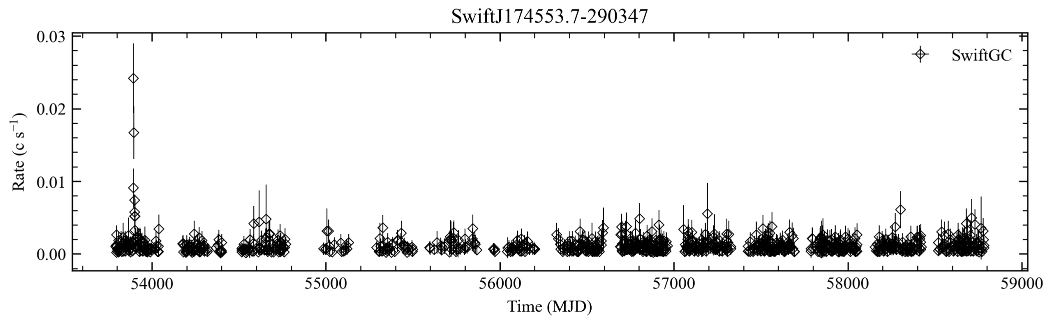
SwiftJ174553.7-290347
SwiftGC
Rate (c s^{-1})
Time (MJD)

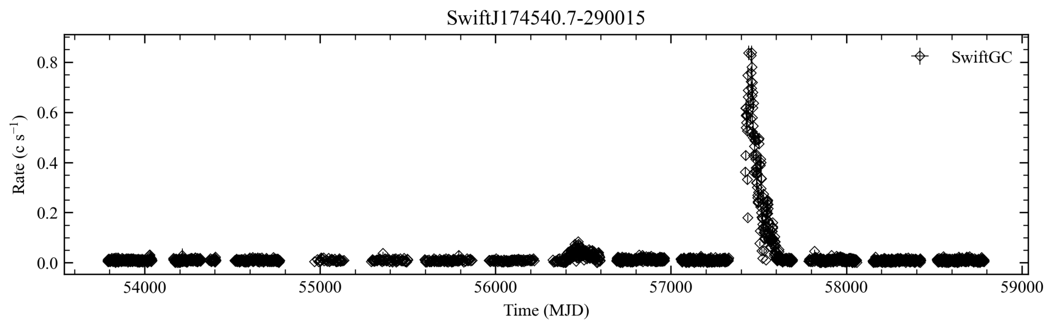
SwiftJ174540.7-290015
SwiftGC
Rate (c s^{-1})
Time (MJD)

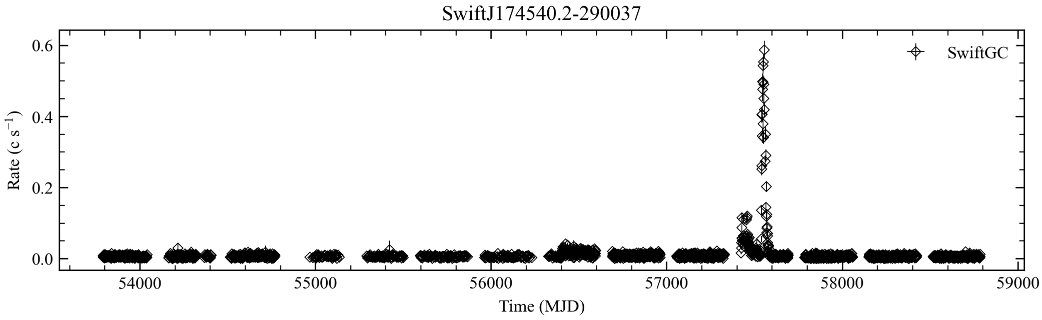
SwiftJ174540.2-290037
SwiftGC
Rate (c s^{-1})
Time (MJD)

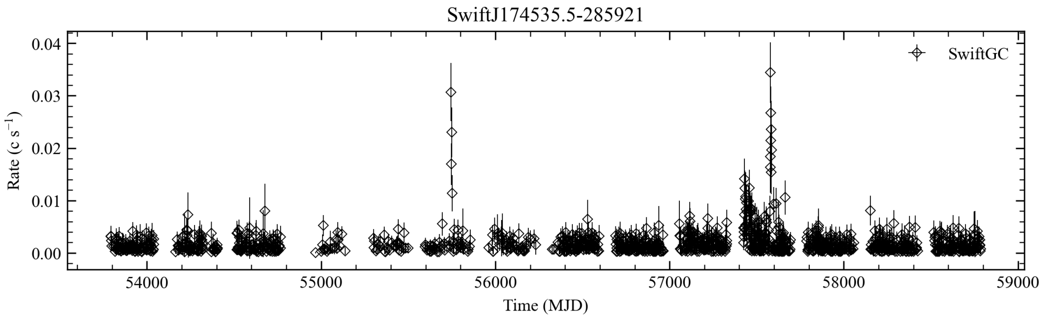
SwiftJ174535.5-285921
SwiftGC
Rate (c s^{-1})
Time (MJD)

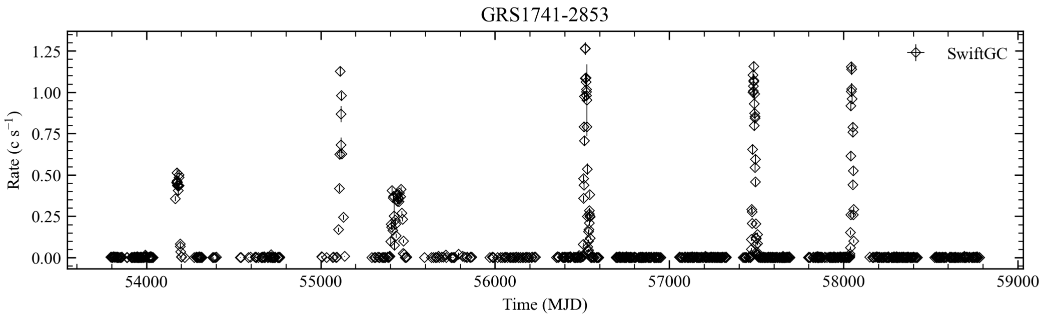
GRS1741-2853
SwiftGC
Rate (c s^{-1})
Time (MJD)

8.2 Gaussian fits

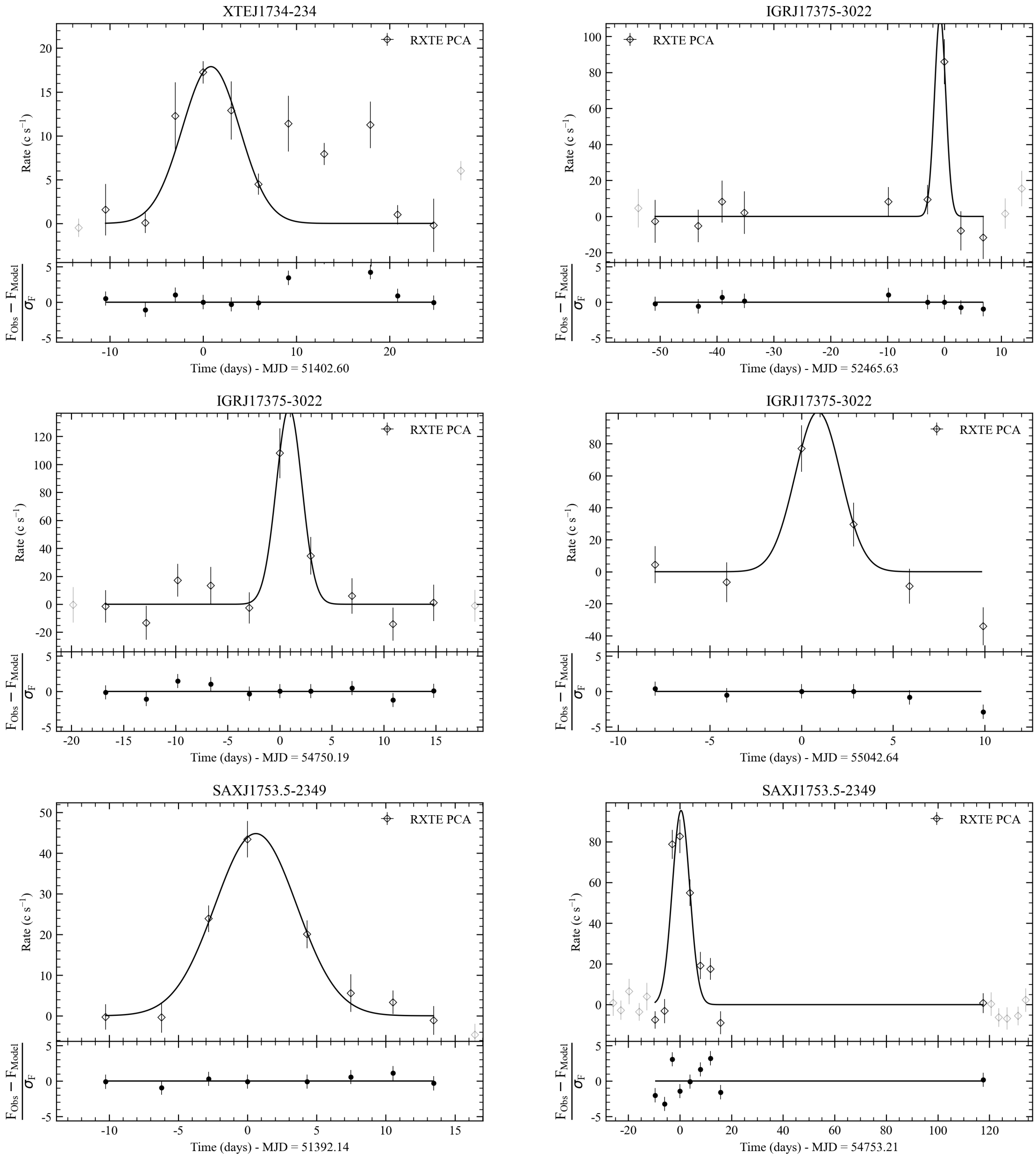

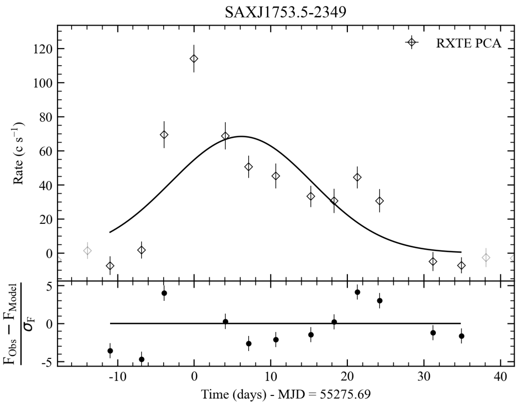
SAXJ1753.5-2349
RXTE PCA
Rate (c s^{-1})
$\frac{F_{Obs} - F_{Model}}{\sigma_F}$
Time (days) - MJD = 55275.69

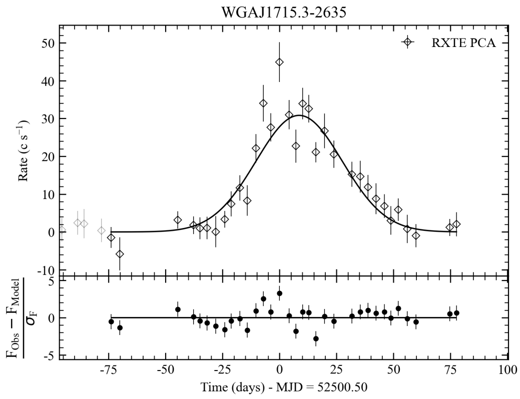
WGAJ1715.3-2635
RXTE PCA
Rate (c s^{-1})
$\frac{F_{Obs} - F_{Model}}{\sigma_F}$
Time (days) - MJD = 52500.50

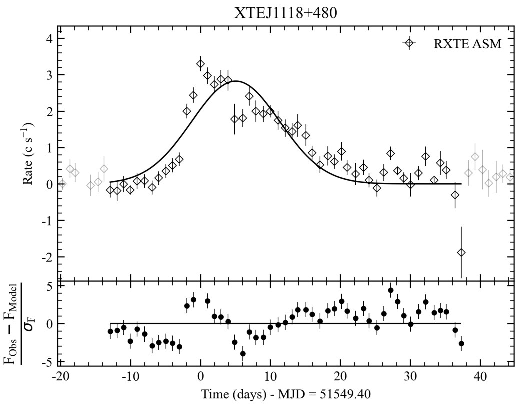
XTEJ1118+480
RXTE ASM
Rate (c s^{-1})
$\frac{F_{Obs} - F_{Model}}{\sigma_F}$
Time (days) - MJD = 51549.40

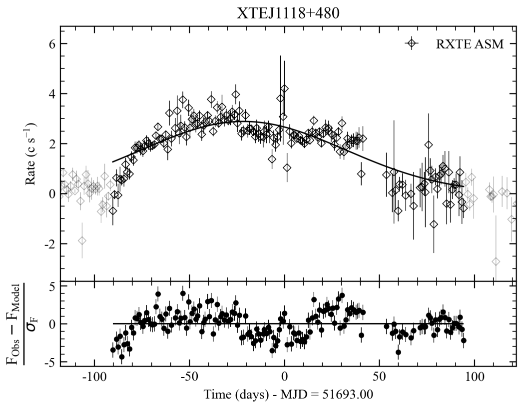
XTEJ1118+480
RXTE ASM
Rate (c s^{-1})
$\frac{F_{Obs} - F_{Model}}{\sigma_F}$
Time (days) - MJD = 51693.00

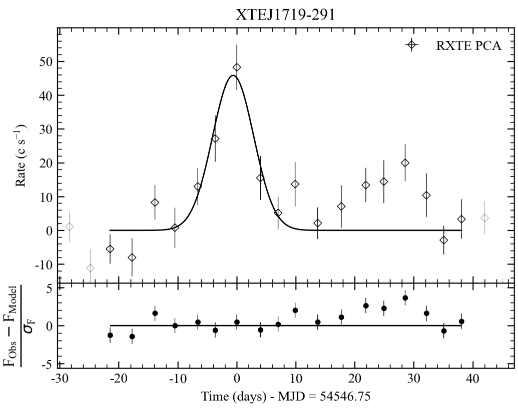
XTEJ1719-291
RXTE PCA
Rate (c s^{-1})
$\frac{F_{Obs} - F_{Model}}{\sigma_F}$
Time (days) - MJD = 54546.75

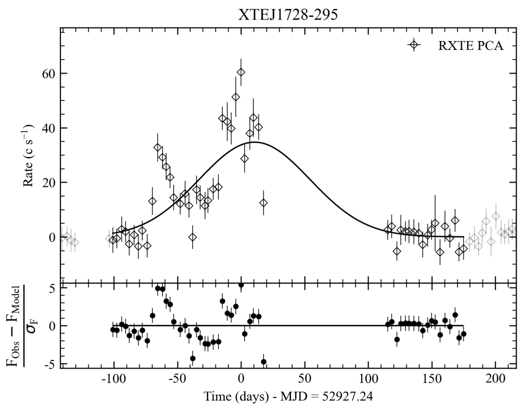
XTEJ1728-295
RXTE PCA
Rate (c s^{-1})
$\frac{F_{Obs} - F_{Model}}{\sigma_F}$
Time (days) - MJD = 52927.24

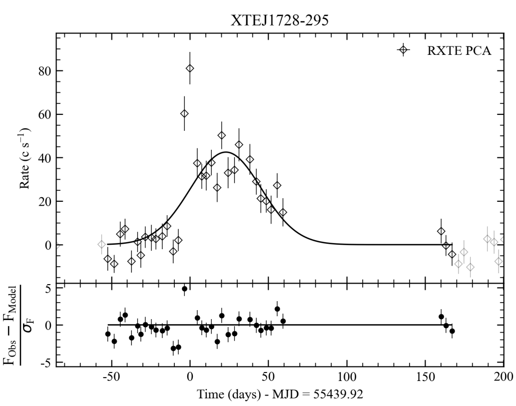
XTEJ1728-295
RXTE PCA
Rate (c s^{-1})
$\frac{F_{Obs} - F_{Model}}{\sigma_F}$
Time (days) - MJD = 55439.92

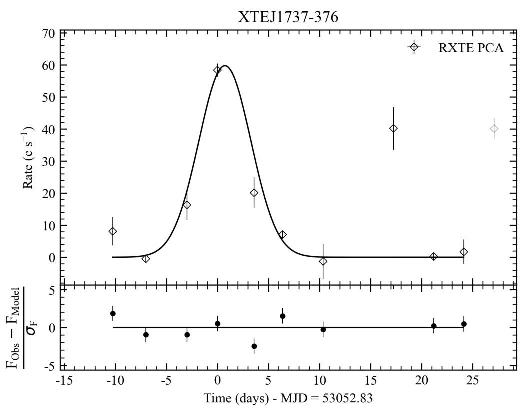
XTEJ1737-376
RXTE PCA
Rate (c s^{-1})
$\frac{F_{Obs} - F_{Model}}{\sigma_F}$
Time (days) - MJD = 53052.83

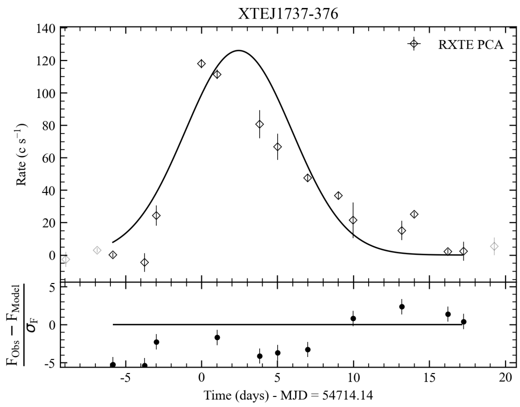
XTEJ1737-376
RXTE PCA
Rate (c s^-1)
F_Obs − F_Model / σ_F
Time (days) - MJD = 54714.14

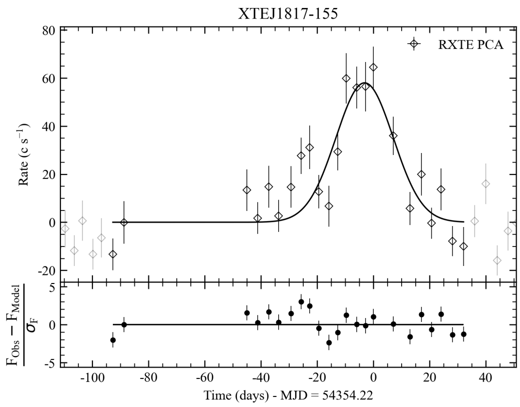
XTEJ1817-155
RXTE PCA
Rate (c s^-1)
F_Obs − F_Model / σ_F
Time (days) - MJD = 54354.22

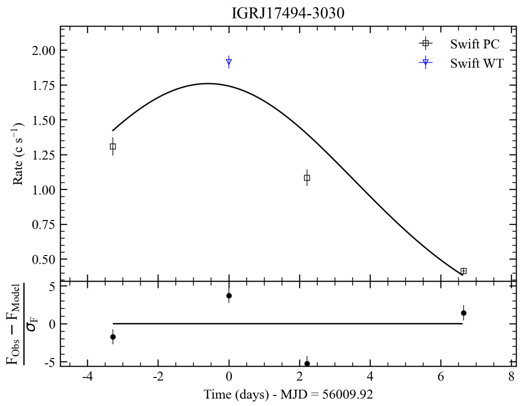
IGRJ17494-3030
Swift PC
Swift WT
Rate (c s^-1)
F_Obs − F_Model / σ_F
Time (days) - MJD = 56009.92

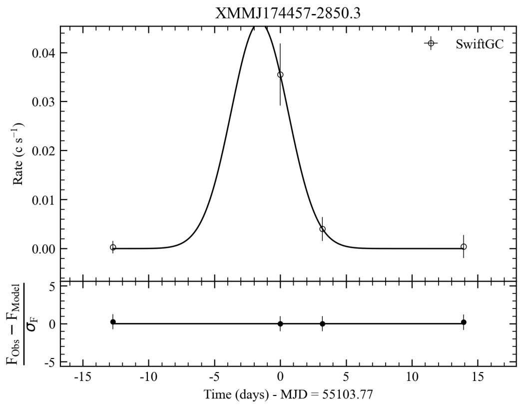
XMMJ174457-2850.3
SwiftGC
Rate (c s^-1)
F_Obs − F_Model / σ_F
Time (days) - MJD = 55103.77

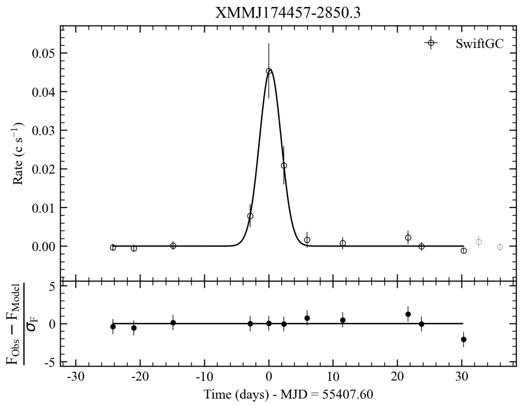
XMMJ174457-2850.3
SwiftGC
Rate (c s^-1)
F_Obs − F_Model / σ_F
Time (days) - MJD = 55407.60

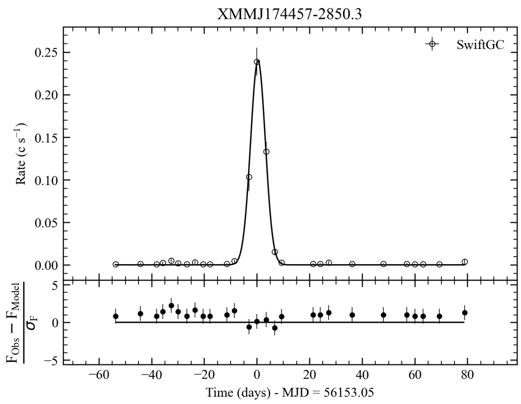
XMMJ174457-2850.3
SwiftGC
Rate (c s^-1)
F_Obs − F_Model / σ_F
Time (days) - MJD = 56153.05

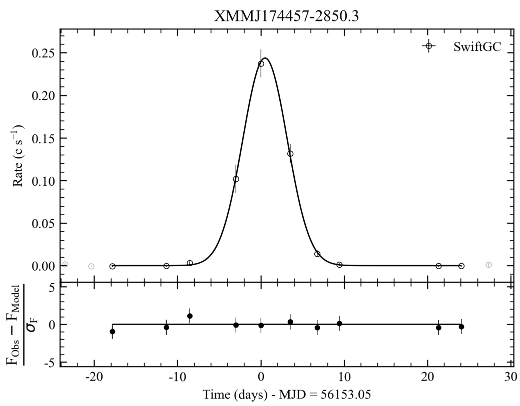
XMMJ174457-2850.3
SwiftGC
Rate (c s^-1)
F_Obs − F_Model / σ_F
Time (days) - MJD = 56153.05

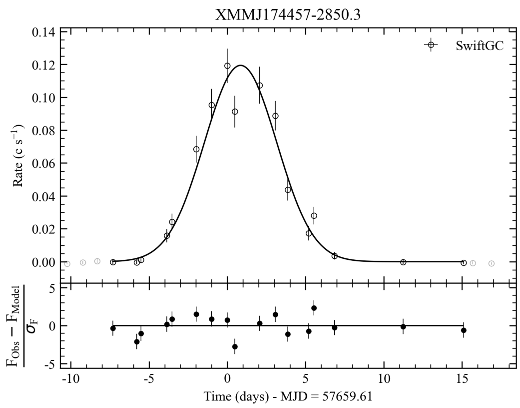
XMMJ174457-2850.3
SwiftGC
Rate (c s^-1)
F_Obs − F_Model / σ_F
Time (days) - MJD = 57659.61

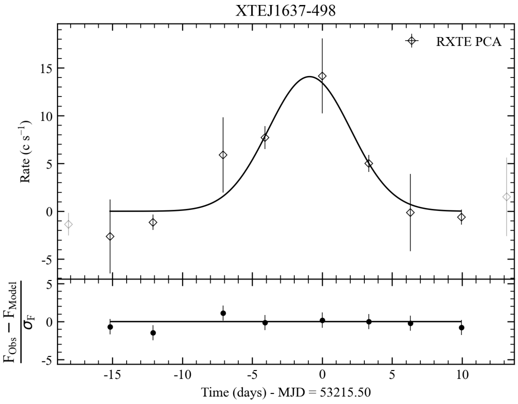
XTEJ1637-498
RXTE PCA
Rate (c s⁻¹)
Time (days) - MJD = 53215.50

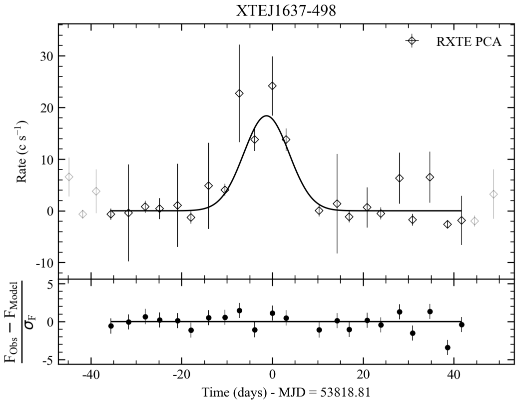
XTEJ1637-498
RXTE PCA
Rate (c s⁻¹)
Time (days) - MJD = 53818.81

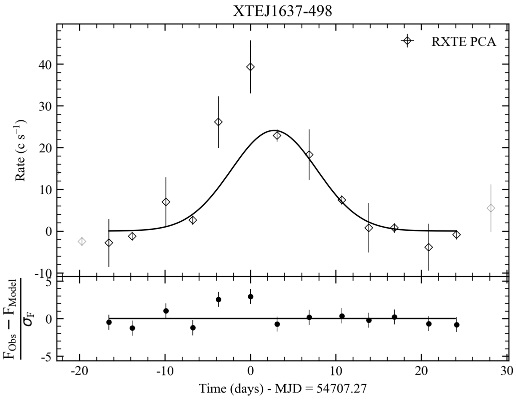
XTEJ1637-498
RXTE PCA
Rate (c s⁻¹)
Time (days) - MJD = 54707.27

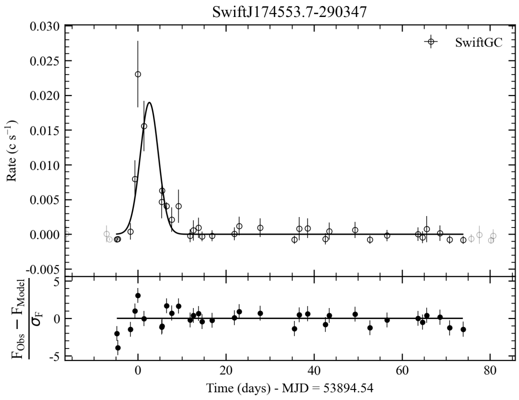
SwiftJ174553.7-290347
SwiftGC
Rate (c s⁻¹)
Time (days) - MJD = 53894.54

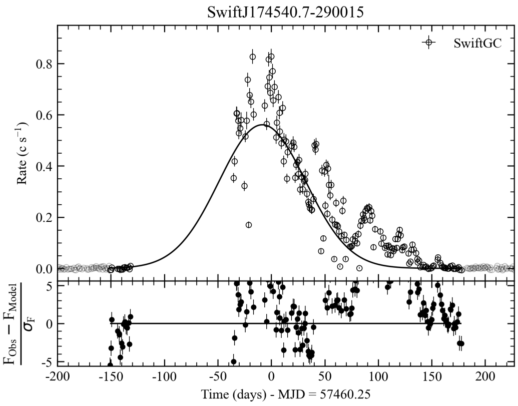
SwiftJ174540.7-290015
SwiftGC
Rate (c s⁻¹)
Time (days) - MJD = 57460.25

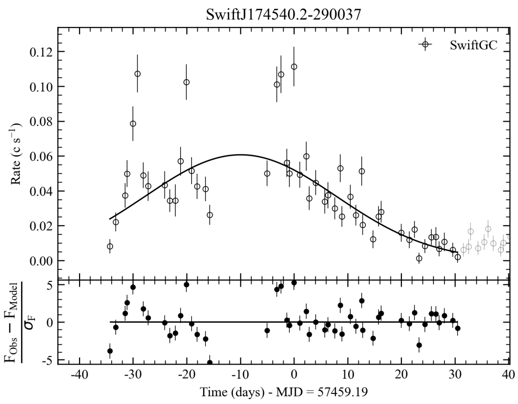
SwiftJ174540.2-290037
SwiftGC
Rate (c s⁻¹)
Time (days) - MJD = 57459.19

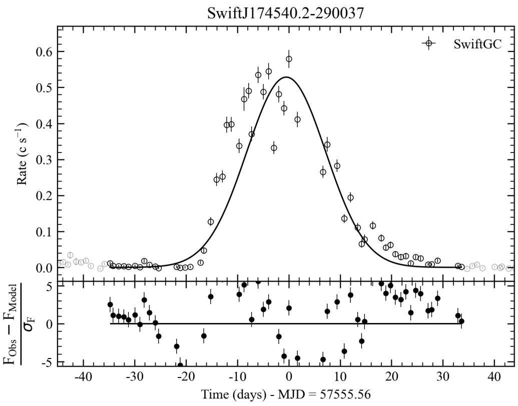
SwiftJ174540.2-290037
SwiftGC
Rate (c s⁻¹)
Time (days) - MJD = 57555.56

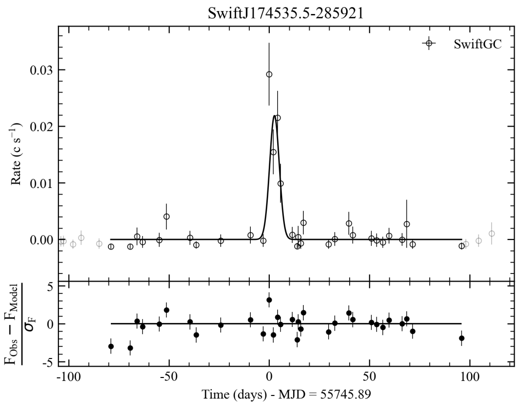
SwiftJ174535.5-285921
SwiftGC
Rate (c s⁻¹)
Time (days) - MJD = 55745.89

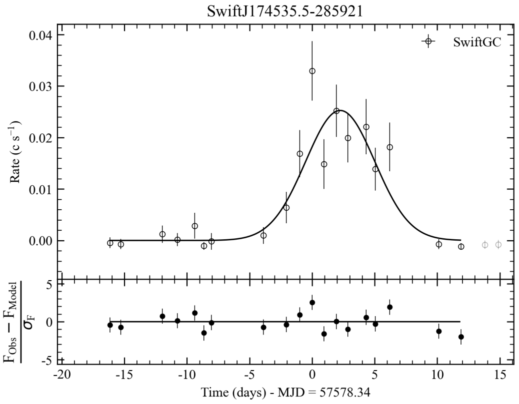
SwiftJ174535.5-285921
SwiftGC
Rate (c s^{-1})
$\frac{F_{Obs} - F_{Model}}{\sigma_F}$
Time (days) - MJD = 57578.34

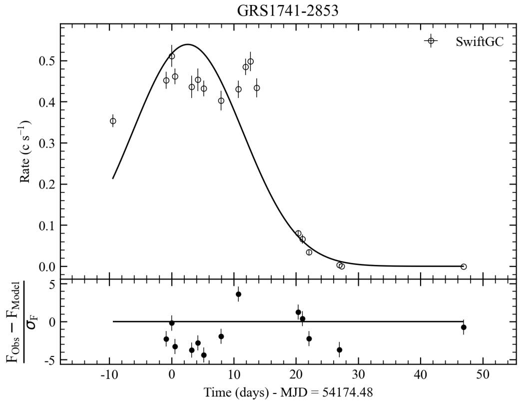
GRS1741-2853
SwiftGC
Rate (c s^{-1})
$\frac{F_{Obs} - F_{Model}}{\sigma_F}$
Time (days) - MJD = 54174.48

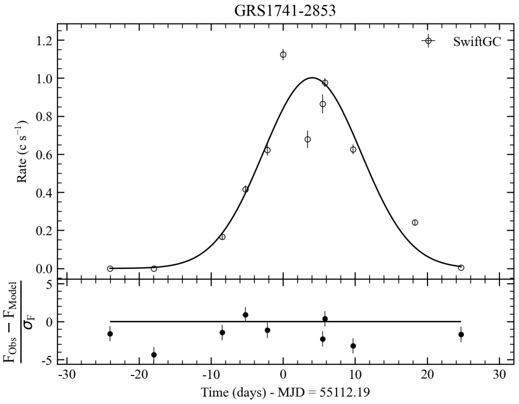
GRS1741-2853
SwiftGC
Rate (c s^{-1})
$\frac{F_{Obs} - F_{Model}}{\sigma_F}$
Time (days) - MJD = 55112.19

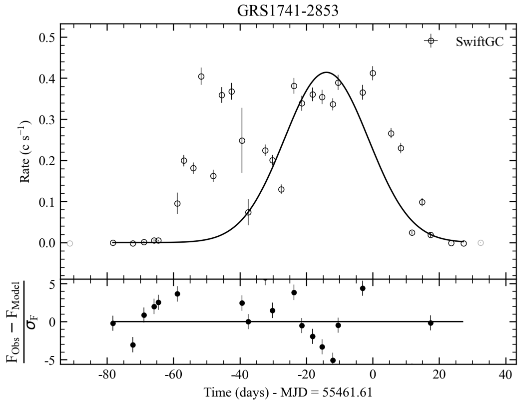
GRS1741-2853
SwiftGC
Rate (c s^{-1})
$\frac{F_{Obs} - F_{Model}}{\sigma_F}$
Time (days) - MJD = 55461.61

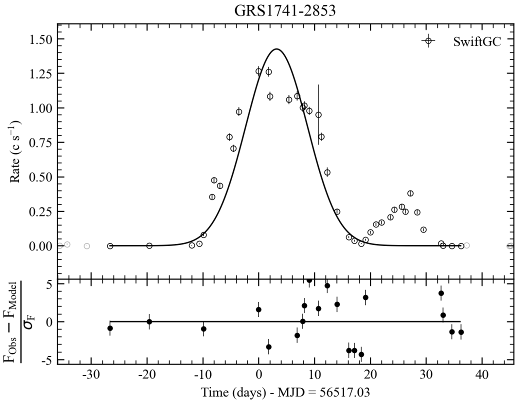
GRS1741-2853
SwiftGC
Rate (c s^{-1})
$\frac{F_{Obs} - F_{Model}}{\sigma_F}$
Time (days) - MJD = 56517.03

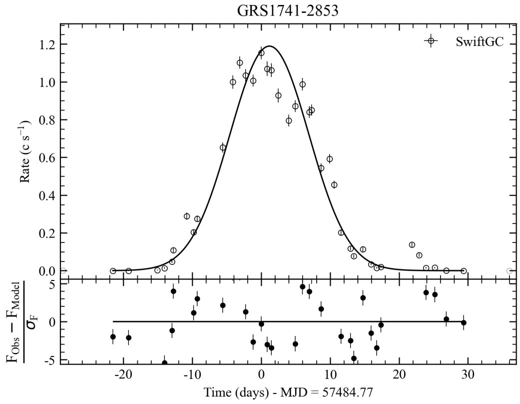
GRS1741-2853
SwiftGC
Rate (c s^{-1})
$\frac{F_{Obs} - F_{Model}}{\sigma_F}$
Time (days) - MJD = 57484.77

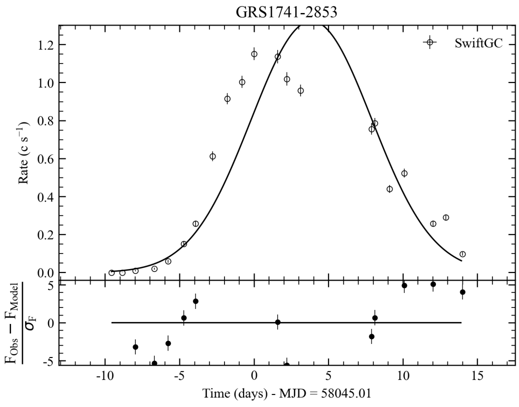
GRS1741-2853
SwiftGC
Rate (c s^{-1})
$\frac{F_{Obs} - F_{Model}}{\sigma_F}$
Time (days) - MJD = 58045.01

8.3 Exponential fits

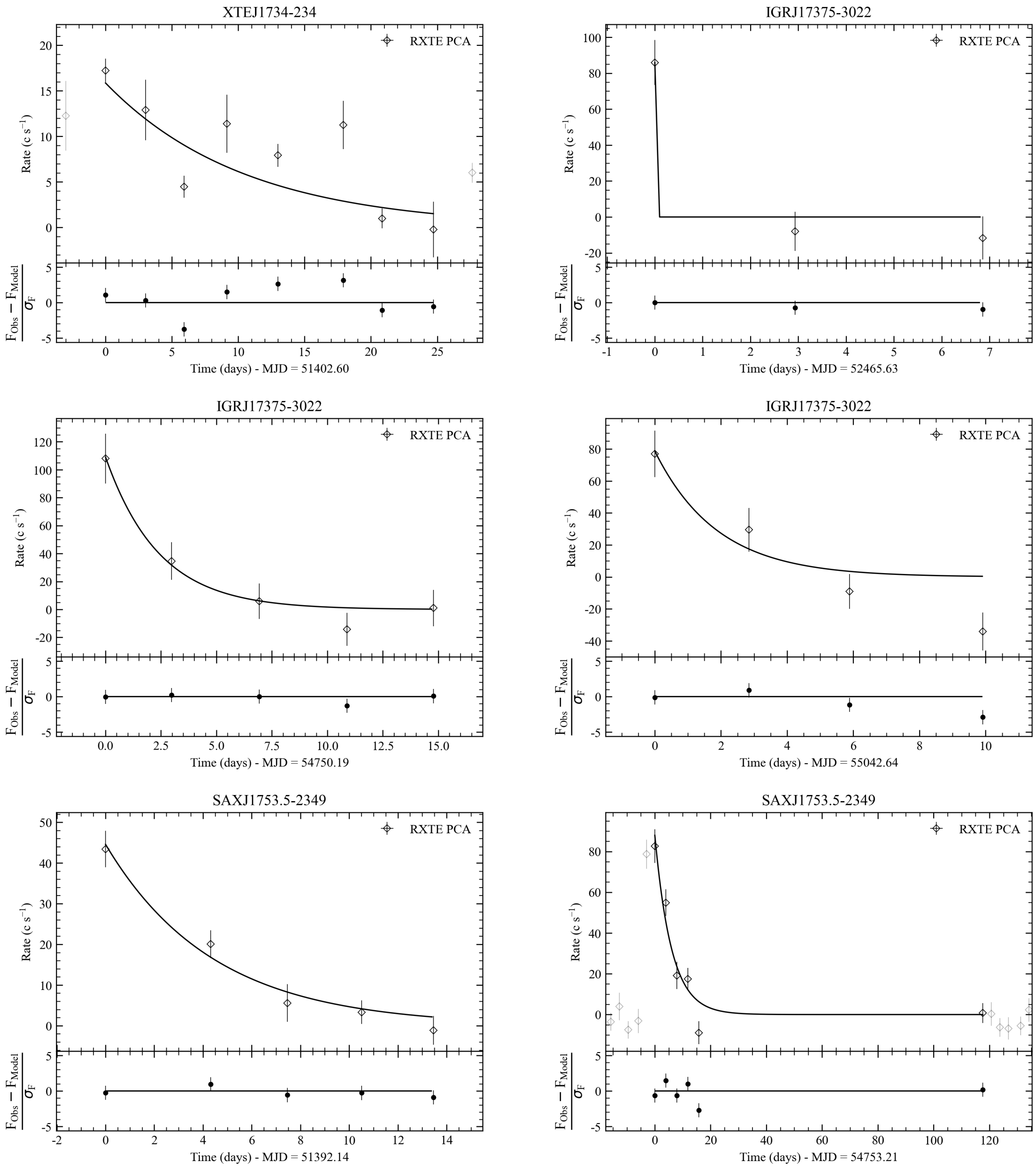

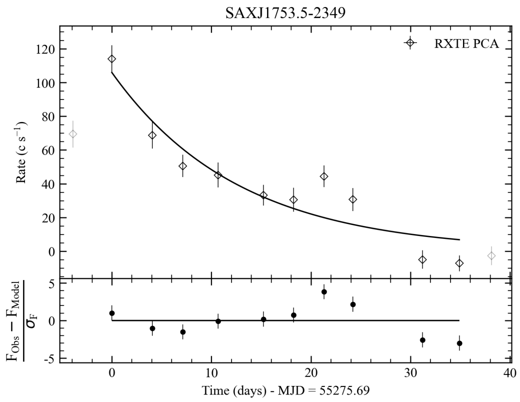
SAXJ1753.5-2349
RXTE PCA
Rate (c s^{-1})
$\frac{F_{Obs} - F_{Model}}{\sigma_F}$
Time (days) - MJD = 55275.69

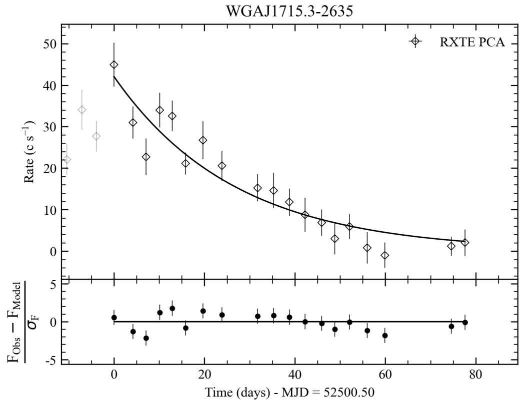
WGAJ1715.3-2635
RXTE PCA
Rate (c s^{-1})
$\frac{F_{Obs} - F_{Model}}{\sigma_F}$
Time (days) - MJD = 52500.50

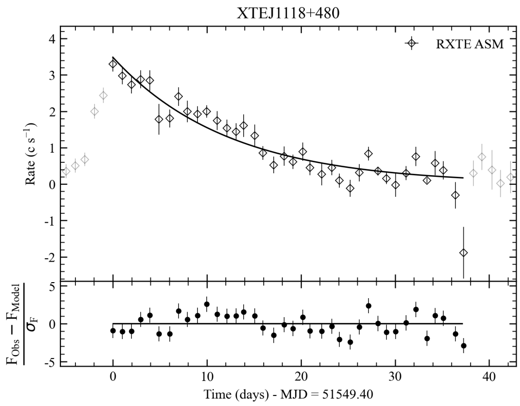
XTEJ1118+480
RXTE ASM
Rate (c s^{-1})
$\frac{F_{Obs} - F_{Model}}{\sigma_F}$
Time (days) - MJD = 51549.40

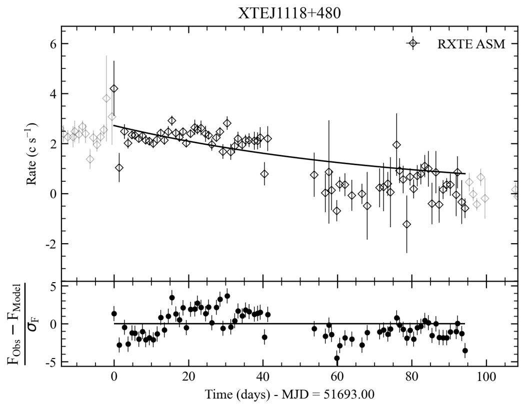
XTEJ1118+480
RXTE ASM
Rate (c s^{-1})
$\frac{F_{Obs} - F_{Model}}{\sigma_F}$
Time (days) - MJD = 51693.00

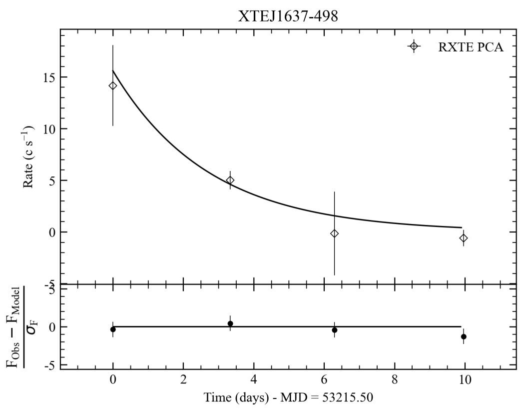
XTEJ1637-498
RXTE PCA
Rate (c s^{-1})
$\frac{F_{Obs} - F_{Model}}{\sigma_F}$
Time (days) - MJD = 53215.50

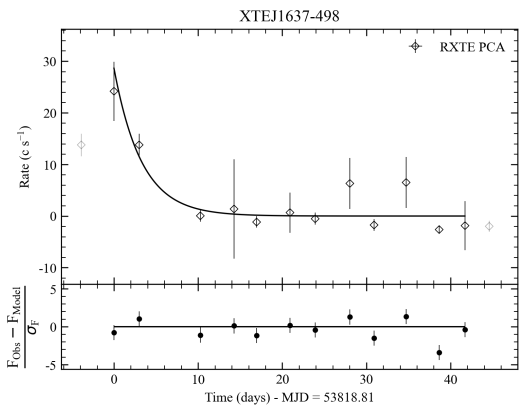
XTEJ1637-498
RXTE PCA
Rate (c s^{-1})
$\frac{F_{Obs} - F_{Model}}{\sigma_F}$
Time (days) - MJD = 53818.81

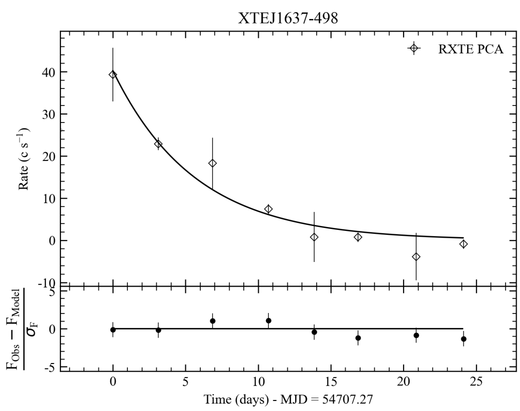
XTEJ1637-498
RXTE PCA
Rate (c s^{-1})
$\frac{F_{Obs} - F_{Model}}{\sigma_F}$
Time (days) - MJD = 54707.27

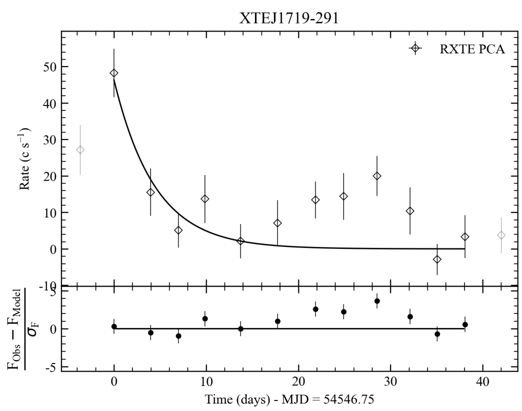
XTEJ1719-291
RXTE PCA
Rate (c s^{-1})
$\frac{F_{Obs} - F_{Model}}{\sigma_F}$
Time (days) - MJD = 54546.75

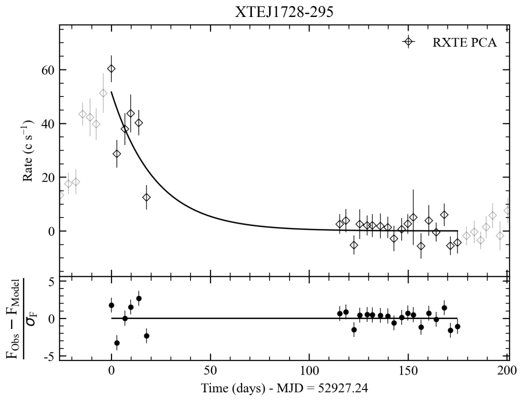
XTEJ1728-295
RXTE PCA
Rate (c s^{-1})
$\frac{F_{Obs} - F_{Model}}{\sigma_F}$
Time (days) - MJD = 52927.24

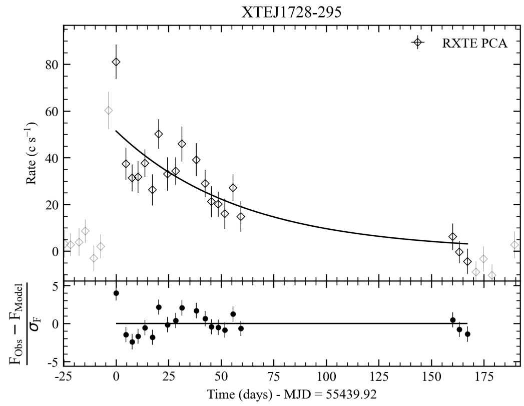
XTEJ1728-295
RXTE PCA
Rate (c s^{-1})
$\frac{F_{Obs} - F_{Model}}{\sigma_F}$
Time (days) - MJD = 55439.92

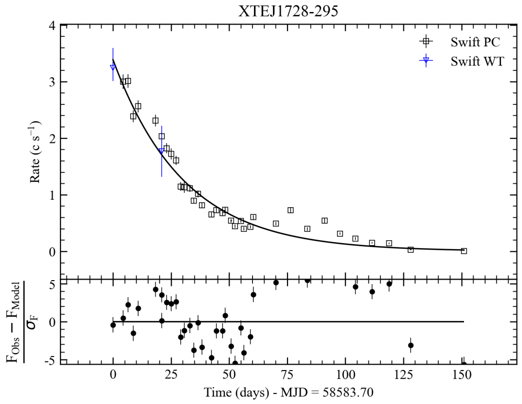
XTEJ1728-295
Swift PC
Swift WT
Rate (c s^{-1})
$\frac{F_{Obs} - F_{Model}}{\sigma_F}$
Time (days) - MJD = 58583.70

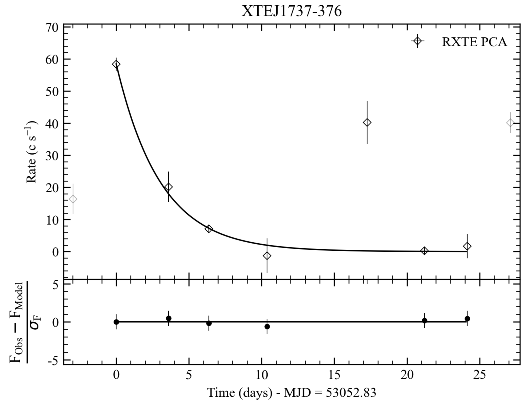
XTEJ1737-376
RXTE PCA
Rate (c s^{-1})
$\frac{F_{Obs} - F_{Model}}{\sigma_F}$
Time (days) - MJD = 53052.83

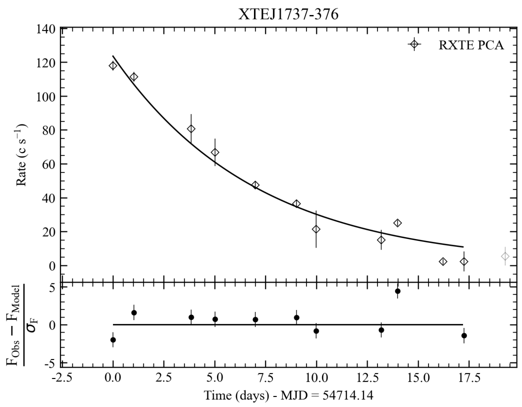
XTEJ1737-376
RXTE PCA
Rate (c s^{-1})
$\frac{F_{Obs} - F_{Model}}{\sigma_F}$
Time (days) - MJD = 54714.14

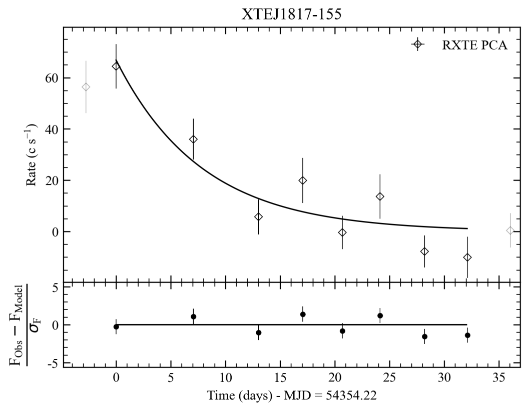
XTEJ1817-155
RXTE PCA
Rate (c s^{-1})
$\frac{F_{Obs} - F_{Model}}{\sigma_F}$
Time (days) - MJD = 54354.22

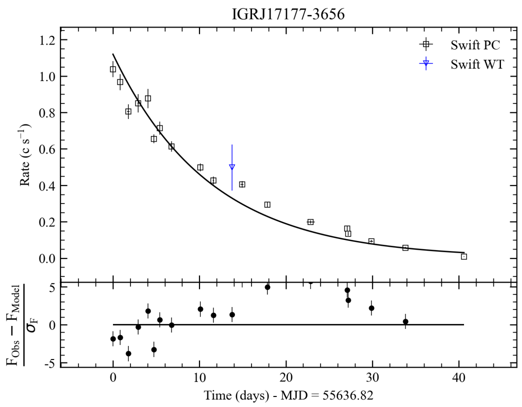
IGRJ17177-3656
Swift PC
Swift WT
Rate (c s^{-1})
$\frac{F_{Obs} - F_{Model}}{\sigma_F}$
Time (days) - MJD = 55636.82

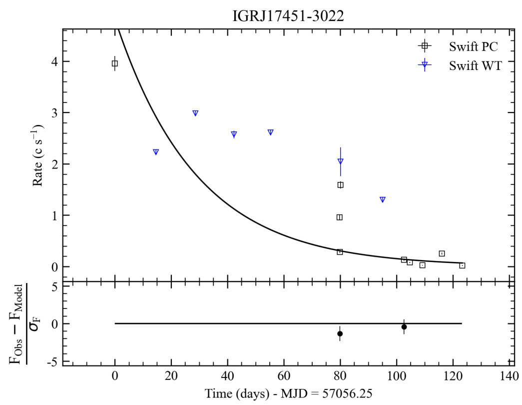
IGRJ17451-3022
Swift PC
Swift WT
Rate (c s^{-1})
$\frac{F_{Obs} - F_{Model}}{\sigma_F}$
Time (days) - MJD = 57056.25

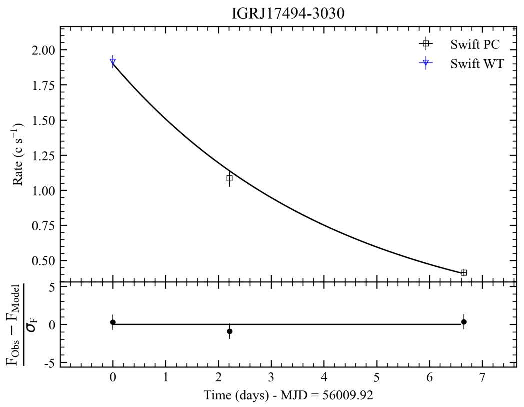
IGRJ17494-3030
Swift PC
Swift WT
Rate (c s^{-1})
$\frac{F_{Obs} - F_{Model}}{\sigma_F}$
Time (days) - MJD = 56009.92

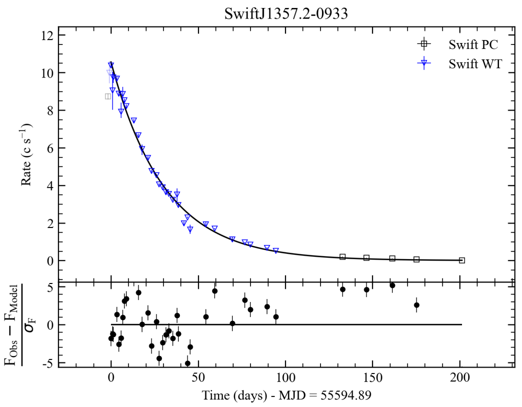
SwiftJ1357.2-0933
Swift PC
Swift WT
Rate (c s^{-1})
$\frac{F_{Obs} - F_{Model}}{\sigma_F}$
Time (days) - MJD = 55594.89

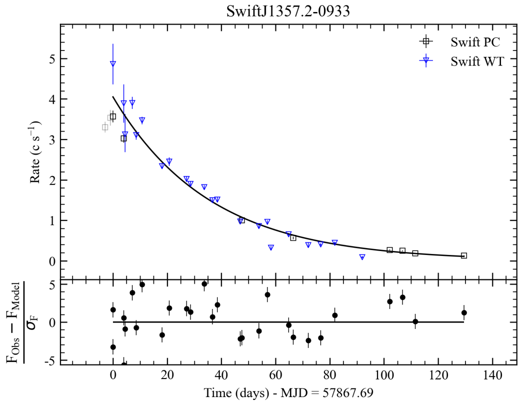
SwiftJ1357.2-0933
Swift PC
Swift WT
Rate (c s^{-1})
$\frac{F_{Obs} - F_{Model}}{\sigma_F}$
Time (days) - MJD = 57867.69

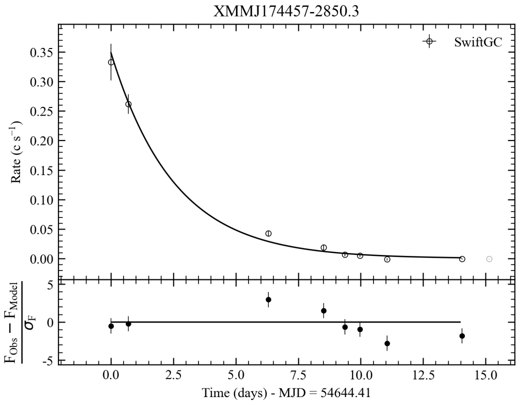
XMMJ174457-2850.3
SwiftGC
Rate (c s^{-1})
$\frac{F_{Obs} - F_{Model}}{\sigma_F}$
Time (days) - MJD = 54644.41

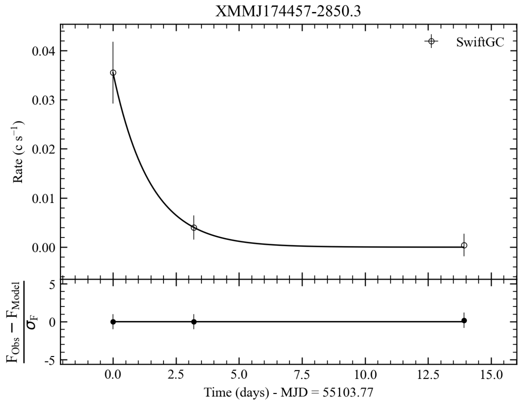
XMMJ174457-2850.3
SwiftGC
Rate (c s^{-1})
$\frac{F_{Obs} - F_{Model}}{\sigma_F}$
Time (days) - MJD = 55103.77

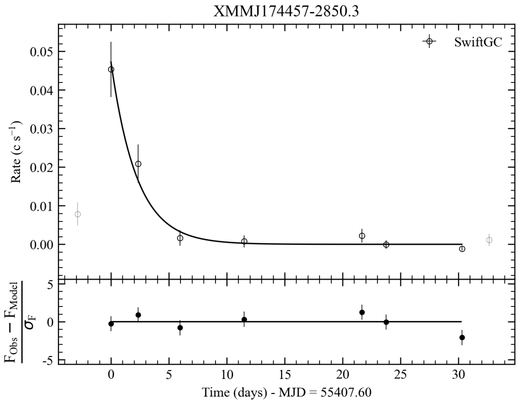
XMMJ174457-2850.3
SwiftGC
Rate (c s^{-1})
$\frac{F_{Obs} - F_{Model}}{\sigma_F}$
Time (days) - MJD = 55407.60

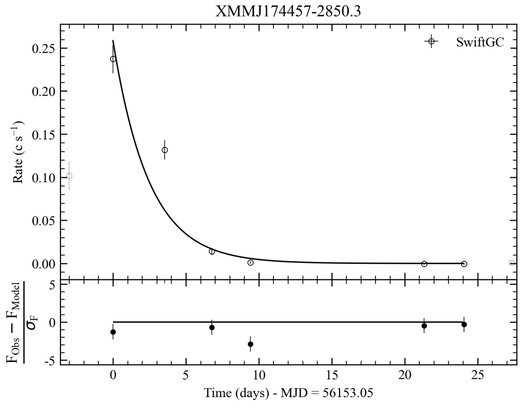
XMMJ174457-2850.3
SwiftGC
Rate (c s^{-1})
$\frac{F_{Obs} - F_{Model}}{\sigma_F}$
Time (days) - MJD = 56153.05

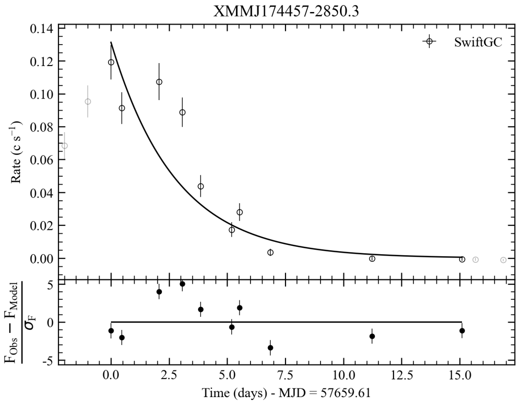
XMMJ174457-2850.3
SwiftGC
Rate (c s^{-1})
$\frac{F_{Obs} - F_{Model}}{\sigma_F}$
Time (days) - MJD = 57659.61

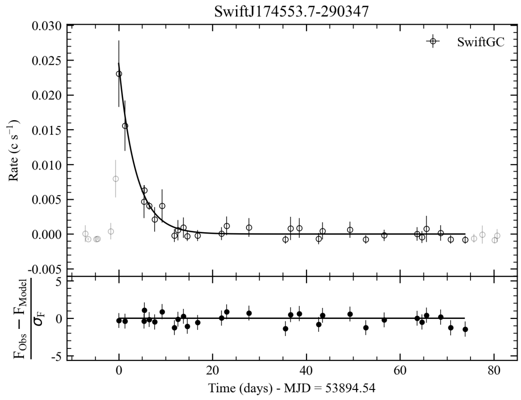
SwiftJ174553.7-290347
SwiftGC
Rate (c s⁻¹)
Time (days) - MJD = 53894.54

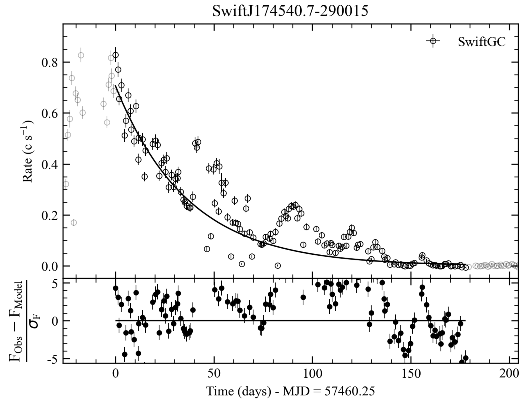
SwiftJ174540.7-290015
SwiftGC
Rate (c s⁻¹)
Time (days) - MJD = 57460.25

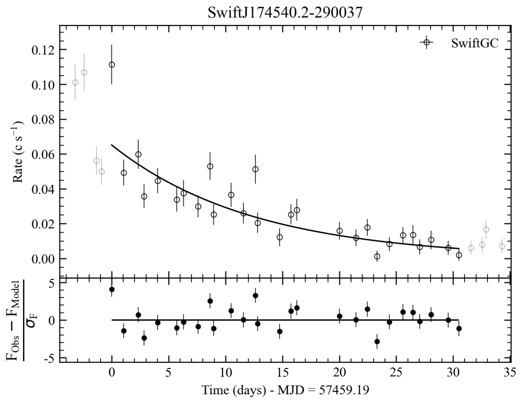
SwiftJ174540.2-290037
SwiftGC
Rate (c s⁻¹)
Time (days) - MJD = 57459.19

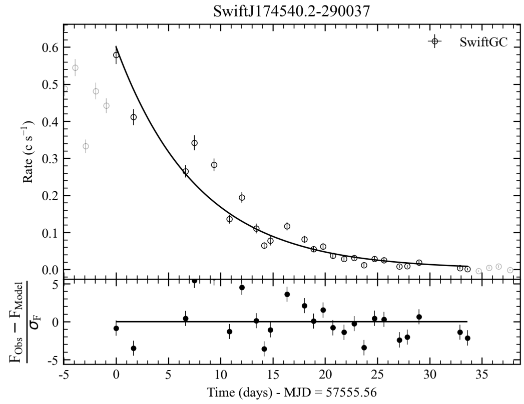
SwiftJ174540.2-290037
SwiftGC
Rate (c s⁻¹)
Time (days) - MJD = 57555.56

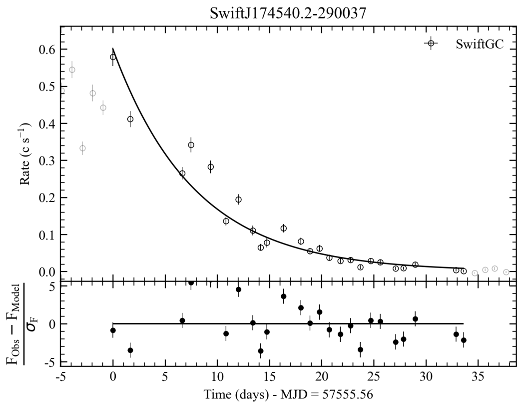
SwiftJ174540.2-290037
SwiftGC
Rate (c s⁻¹)
Time (days) - MJD = 57555.56

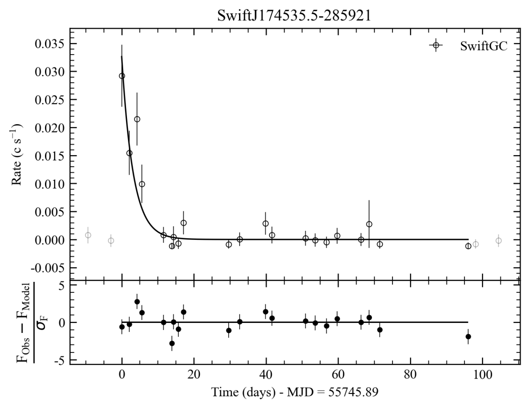
SwiftJ174535.5-285921
SwiftGC
Rate (c s⁻¹)
Time (days) - MJD = 55745.89

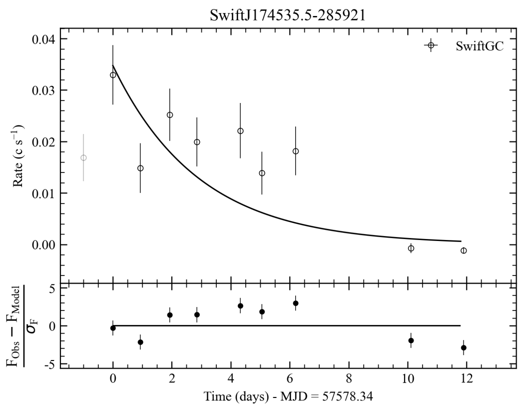
SwiftJ174535.5-285921
SwiftGC
Rate (c s⁻¹)
Time (days) - MJD = 57578.34

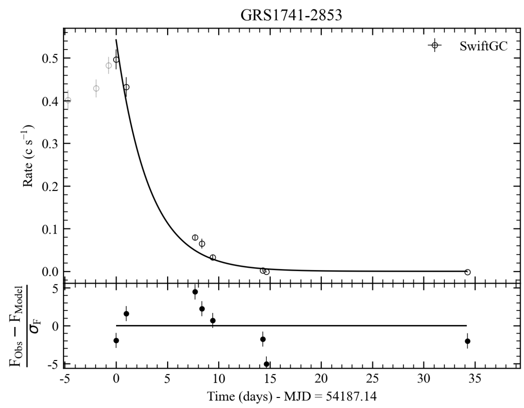
GRS1741-2853
SwiftGC
Rate (c s⁻¹)
Time (days) - MJD = 54187.14

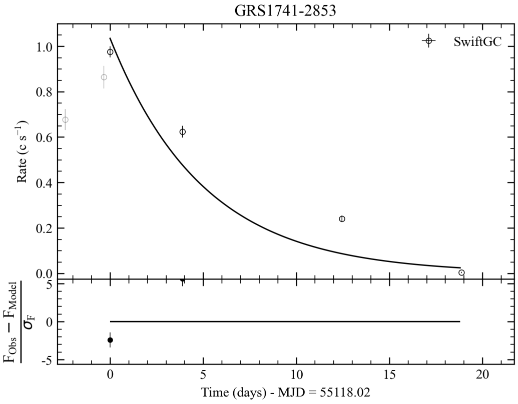
GRS1741-2853
SwiftGC
Rate (c s⁻¹)
(F_Obs − F_Model)/σ_F
Time (days) - MJD = 55118.02

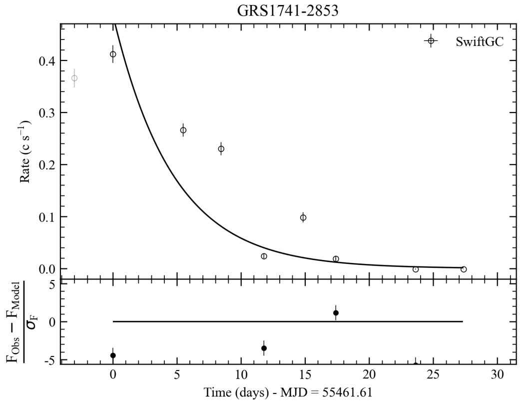
GRS1741-2853
SwiftGC
Rate (c s⁻¹)
(F_Obs − F_Model)/σ_F
Time (days) - MJD = 55461.61

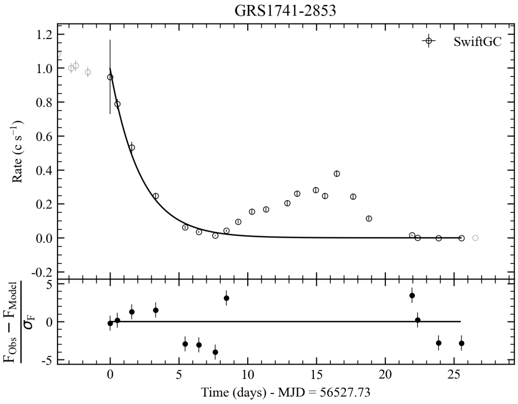
GRS1741-2853
SwiftGC
Rate (c s⁻¹)
(F_Obs − F_Model)/σ_F
Time (days) - MJD = 56527.73

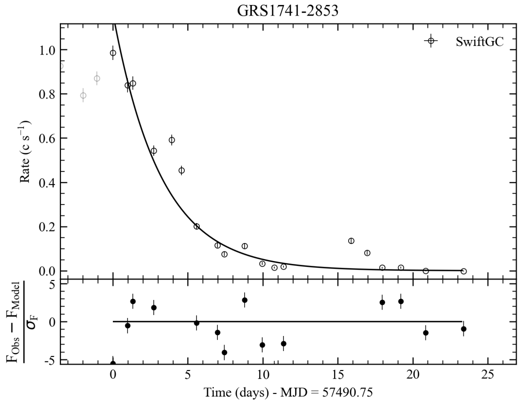
GRS1741-2853
SwiftGC
Rate (c s⁻¹)
(F_Obs − F_Model)/σ_F
Time (days) - MJD = 57490.75

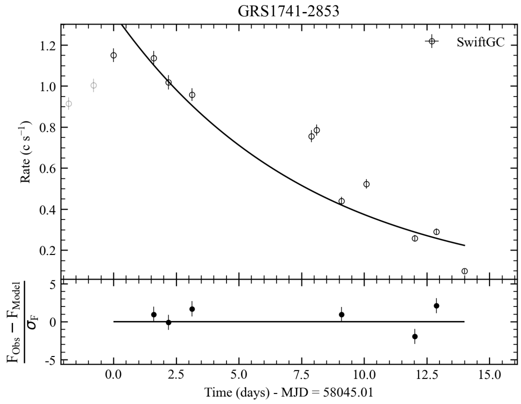
GRS1741-2853
SwiftGC
Rate (c s⁻¹)
(F_Obs − F_Model)/σ_F
Time (days) - MJD = 58045.01